Kaunas University of Technology

Mechanical Engineering and Design

Analysis of adhesive bonding in carbon fiber bar single lap and double lap joints

Master's Final Degree Project

Naga Manikanta Kommanaboina

Project author

Assoc. Prof . Dr Paulus Griskevicius

Supervisor

Kaunas, 2019

Kaunas University of Technology

FACULTY OF MECHANICAL ENGINEERING AND DESIGN

Master's Final Degree Project

Analysis of adhesive bonding in carbon fiber bar single lap and double lap joints

Naga Manikanta Kommanaboina

Project author

Assoc. Prof.Dr. Paulus Griskevicius

Supervisor

Assoc.Prof, Valdas Eidukynas.

Reviewer

Kaunas, 2019

Kaunas University of Technology
FACULTY OF MECHANICAL ENGINEERING AND DESIGN

Naga Manikanta Kommanaboina

Analysis of adhesive bonding in carbon fiber bar single lap and double lap joints

Declaration of Academic Integrity

I confirm that the final project of mine, Naga Manikanta Kommanaboina, on the topic,‘‘Analysis of adhesive bonding in carbon fiber bar single lap and double lap joints’’ is written completely by my self; all the provided data and research results are correct and have been obtained honestly. None of the parts of this thesis have been plagiarized from any printed, Internet-based or otherwise recorded sources. All direct and indirect quotations from external resources are indicated in the list of references. No monetary funds (unless required by Law) have been paid to anyone for any contribution to this project.

I fully and completed understand that any discovery of any manifestations/case/facts of dishonesty inevitably results in me incurring a penalty according to the procedure(s) effective at Kaunas University of Technology.

(name and surname filled in by hand) (signature)

Kaunas University of Technology

Faculty of Mechanical Engineering and Design

Study Programme – Aeronautical Engineering 6211EX024

Task Assignment for Final Degree Project of Master Studies

Student: Naga Manikanta Kommanaboina

1. Title of the Final Project:

Analysis of adhesive bonding in carbon fiber bar single lap and double lap joints

Anglies pluošto strypelių vienpusio ir dvipusio sujungimo adhezijos analizė.

2. Aim of the Final Project:

Investigated the carbon fiber adhesive bond single lap and double lap joints through experimentally and numerically and finding strength and durability, the ultimate strength of the joints.

2. Tasks of the Final Project:

- Construction of the experimental setup for sailplane wing spar for structural analysis
- Numerical calculation using ABAQUS® and MATLAB for adhesive bonding in carbon fiber lap joints
- 3-D analysis of the Finite Element model.
- Comparision of experimental and computational results.

3. Structure of the Text Part:

- Finding the ultimate strength, stiffness, deformation or cracking of adhesive bonding in carbon fiber single lap joint.
- Evaluation of the bonding strength of the carbon fiber rod at different loads and cohesive damage properties.
- Stress-strain plots of the adhesive bonding and deformations of the single bar and double joints.
- Assessment of an alternative method for the determining of the mechanical properties.
- Three-dimensional single lap and balanced and unbalanced double lap joints and finding the influence of the structural adhesive and adherend stress distribution.
- Suggesting the best and stress reduced joints for sailplane spar connection.

4. Consultants of the Final Project:

Author of the Final Project _____

(Name, Surname, Signature, date)

Supervisor of the Final Project _____

(Name, Surname, Signature, date)

Head of Study Programme Janina Jablonskytė

(Name, Surname, Signature, date)

Kommanaboina, Naga Manikanta. Analysis of adhesive bonding in carbon fiber bar single lap and double lap joints. Master's Final Degree Project/supervisor Assoc. Prof. Dr. Paulus Griskevicius; FACULTY OF MECHANICAL ENGINEERING AND DESIGN, Kaunas University of Technology.

Study field and area: Aeronautical Engineering (E14), Engineering Science

Keywords: Carbon fiber adhesion joints, strength, durability, finite element method, Single lap joint, adhesive bonding, deformation, double lap joint, stress distribution, delamination, crack propagation, sailplane spars.

Kaunas, 2019. 67 p.

Summary

The aircraft wing locks are made of carbon fiber roads that are glued to an epoxy resin. Due to the features of joining the wing parts, this examination is intended to form a database of mechanical properties of such of the adhesive bond. Investigated the carbon fiber adhesive joints through experimentally and numerically. The focus is on experimental and quasi-analytic strength adhesive bonding of one-sided and two-sided balanced and unbalanced joints, a few characteristics of the connections such as breaking and adhesive bonding strength, strength and durability of the joints.

The numerical simulations of three-dimensional single lap and balanced and unbalanced double lap joints and finding influences of the structural adhesive and adherend stress distribution, delamination in various regions for suggesting the best and stress reduced joints for sailplane spar connection. Experimental research is a method for determining mechanical properties, but it is very expensive, especially the cyclic loading tests. This justifies the search for alternative methods that require cheaper devices and shortens time costs. The prepared ABAQUS and MATLAB models well describe the strength and durability of the joints and can be used for design and technical diagnostics.

Kommanaboina, Naga Manikanta. Anglies pluošto strypelių vienpusio ir dvipusio sujungimo adhezijos analizė. Magistro baigiamasis projektas / vadovas doc. dr. Paulius Griškevičius; Kauno technologijos universitetas, Mechanikos inžinerijos ir dizaino fakultetas.

Studijų kryptis ir sritis (studijų krypčių grupė): Aviacijos inžinerija (E14), Inžinerijos mokslai.

Reikšminiai žodžiai: anglies pluošto jungtys, stiprumas, baigtinių elementų metodas, vienpusio ir dvipusio sujungimo adhezija, deformacijos, įtempių pasiskirstymas, delaminacija, plyšio augimas, sklandytuvo sparnas.

Kaunas, 2019. 67 p.

Santrauka

Orlaivio sparnų užraktai yra pagaminti iš anglies pluošto strypelių, kurie suklijuojami su epoksidine derva. Dėl sparnų dalių sujungimo ypatybių šis tyrimas skirtas sukurti tokios jungties mechaninių savybių duomenų bazę. Darbe eksperimentiškai ir skaitiniais metodais ištirta anglies pluošto klijų jungtis. Pagrindinis dėmesys skiriamas strypelių vienpusio ir dvipusio sujungimo adhezijos eksperimentinei stiprumo analizei, bei kai kurioms jungčių charakteristikoms, pvz., suirimo ir klijų sukibimo jėgai, jungčių stiprumui tirti.

Erdviniai vienpusio ir dvipusio simetriško ir asimetriško sujungimo skaitmeniniai modeliai su adhezijos vientisumo vertinimu bei įtempių pasiskirstymu leidžia analizuoti pavojingas zonas. Eksperimentiniai tyrimai - tai mechaninių savybių nustatymo metodas, tačiau jis yra labai brangus, ypač cikliniai apkrovos bandymai, todėl svarbūs yra alternatyvūs metodai, kuriems pakanka pigesnių priemonių ir mažiau laiko sąnaudų. Paruošti ABAQUS ir MATLAB modeliai gerai apibūdina sujungimų stiprumą ir ilgaamžiškumą ir gali būti naudojami projektavimui ir techninei diagnostikai.

Table of contents

List of figures

List of tables

List of abbreviations

FEM: Finite element method

DSC: Differential scanning calorimetry

VCCT: Virtual break closure technique

CFC: Carbon fiber composite

FEA: Finite element analysis

GBJM: Global bolt joint model

SHM: Structural health monitoring

CZM: Cohesive zone model

XFEM: Extended finite element method

Introduction

Now a day's aerospace industries are mostly looking for light-weight materials to improve strength has prompted to move from the metal to composite materials, which will give the more strength and durability. Most of the aircraft locks are made of carbon fiber rods that are attached through the epoxy resin. Adhesive bonding joints are more effective than mechanically fixed joints as they perform uniform stress distribution. Since adhesively strengthened joints are strong in shear however fail in the peel. Aircraft design mostly made of carbon fiber composites might be 33% lighter than metal developments. Replacing metal fasteners by using the automated molding process can significantly reduce the cost of manufacturing complex structures. This development of the production of composite structures is a positive sign for the replacement of metal developments by composites [4].

The failure of aircraft components can have catastrophic consequences; the examination and forecast of aircraft failure can avoid loss of life and property damage. Structural and fatigue analysis is used to predict the structure fail when subjected to a cyclic load. This failure occurs due to more stress concentrations. These bonds are exposed to high mechanical weights which prompts the improvement of shear stresses causing debonding the structures. Keeping in mind end goal to make up for these forces, glue with suitable quality must be chosen; in any case, it is critical that selected adhesive has the optimal properties to permit strong and high joint quality [1].

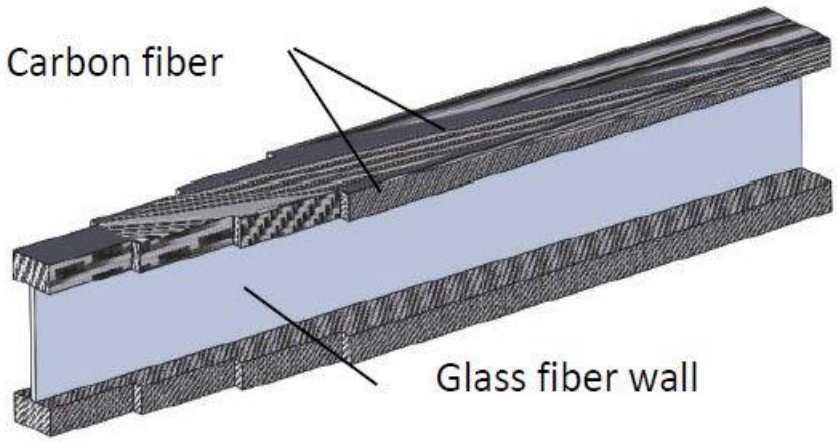

Fig. 1. General view of composite wing spar [1]

The idea of using different types of carbon fiber rod connections as a spar in sail-plane wing and also installing stiffness spar by filling with proper adhesives. Adhesive bonding joints playing a key role in the aerospace, aeronautical and automobile, Packing, marine, and semiconductor industries [1]. Mainly the production and development of composites and carbon fiber joints in aircraft. These glue joints have the ability to replace the conventional fasteners and rivet joints and by applying perfect adhesive material can join large structures. The failure in adhesively bonded joints are pre-dominantly 2 types, which is an adhesive and cohesive failure, it's happening for the most part because of interfacial(glue) cracking, likewise called de-bonding, at geometric limits because of stress concentrations or results from the joints fabrication [5]. Among all other methods, Adhesive

bonding prevents the avoidance of drilling holes and higher stress distribution. Normally double lap joints are simple layout with relatively peel stress. The orthotropic behavior is seen in material and consequently, that needs an uncoupled subject to recognize the failures. The delamination and its development need more prominent contributions in recreation systems including FE plans. The spar is the main purpose of sharing and transferring wing load. Generally, the spars are subjected to transfer loads [2].

The main focus is the numerical analysis influence of the structural adhesive stress distribution in various regions, delamination in three-dimensional various doubles lap and single lap connections. Adhesively bonded joints are progressively being utilized in joining different structural components made of carbon fibers. The emphasis is on experimental and quasi-analytical strength adhesive bond of shear lap and double lap joints, a few characteristics of the connection such as breaking, the strength of the bond. By using these analyses suggesting the best and stress reduced joints for sailplane spar connection. The certain adhesive makes stronger bonds with particular materials and a joint made with an adhesive which does not viably hold fast to the picked material will prompt untimely disappointment. So as to assess the mechanical properties of single lap and double lap shear tests performed in FEA. The experiment was carried on an INSTRON E10000 electromechanical test machine. Adhesive joints are relied upon to hold a noteworthy extent of their heap bearing limit with regards to the whole span of the entire life of the reinforced structure.

1.1. Sources

The following sources were used for this project:

1. Similar work presentation

2. Test books

3. Articles from the journals.

4. Statistical data.

5. Manuals from the product manufacture

6. Reports from scientific and engineering forums

2. Literature review

The adhesives have a long history dating back to ancient times. Initially, adhesives were made based on animal and plant substances. Around 2000 BC adhesives were used in the of the chariot wheels where the wooden spokes were bonded to the rim under compression. Evaluation of adhesive bonding started when N.A de Bruyne and Ryner developed an adhesive based on the combination of polyvinyl formal and phenolic resins. This new adhesive was less brittle and toughness enabling metallic, wooden components are successfully bonded. The development of epoxy adhesives spread further uses in primary structures. After world war 2, the wooden aircraft became obsolete. Wooden structures, like plastic composites, suffer from the adhesive degrading effects of moisture and temperature, delamination and rot. In the 1950s the bonding techniques for aluminum in aircraft structures were fully developed [2].

Fig. 2. Advanced wooden aircraft (De Havilland and Mosquito) [2]

2.1. Composite structures

Composite materials are used broadly in aircraft structures. The primary driver is their weight-saving. Every new generation of aircraft generally uses thicker laminates for carrying more load. The uses of composites in the current airplane are exemplified by a schematic over the new commercial airliners [3].

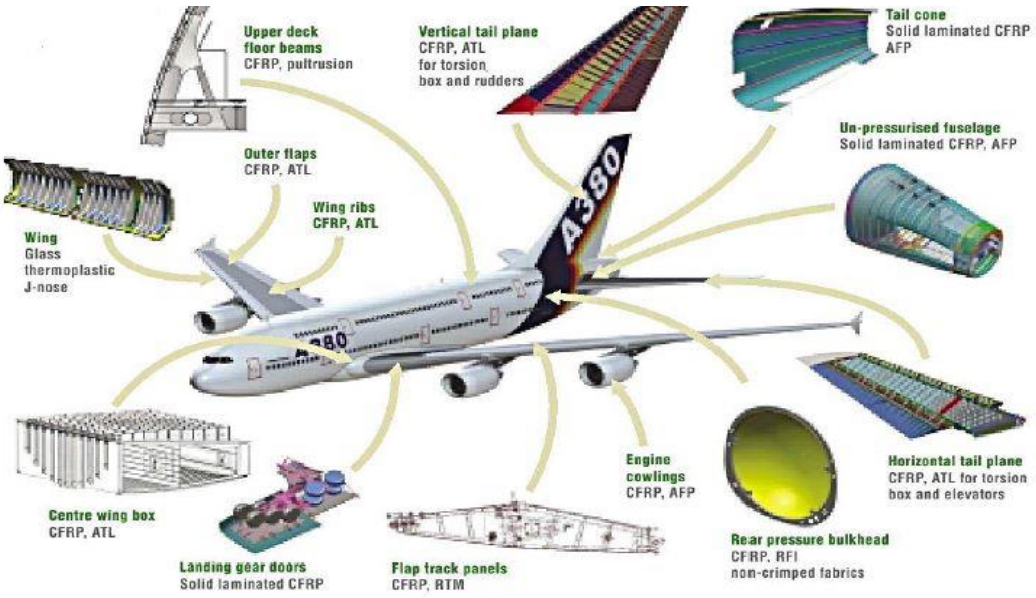

Fig. 3. Major Composite parts on the Aircraft [3]

2.2. Bonded structures

It is utilized to attaching the surfaces and this bonding technics are mainly glues, epoxies, or different types of plastics that attachment by curing with a certain amount of thermal load. Most of the modern glues are carbon-based on petrochemical and the basic bonding procedure can be surface adsorption (intermolecular or inter-atomic fascination powers amongst surface and adhesive), synthetic bonding (van-der-Waals powers, valence bonds), dispersion(interfusion of glue into the structure of polymeric bond accomplices), electrostatic fascination and mechanical interlocking. Adhesives offer the possibility to create new, challenging product designs. Structural and specialty glues represent about 30% of total glue and sealant deals, with uses in many industries; Aerospace, automotive, domestic appliance, mechanical machine, etc. Joint designs which are perfectly fit to other joining methods might be quite unsuitable for adhesives [4]. Glue bonds are taken for the fabrication of composite structures. Evaluating the influence in the geometry of the adhesive and adherends Abaqus software was used to find the mechanical properties of the lap joints. Mostly used cohesive zone models for uniaxial load tensile load tests [13].

2.2.1. Structural bonded joints

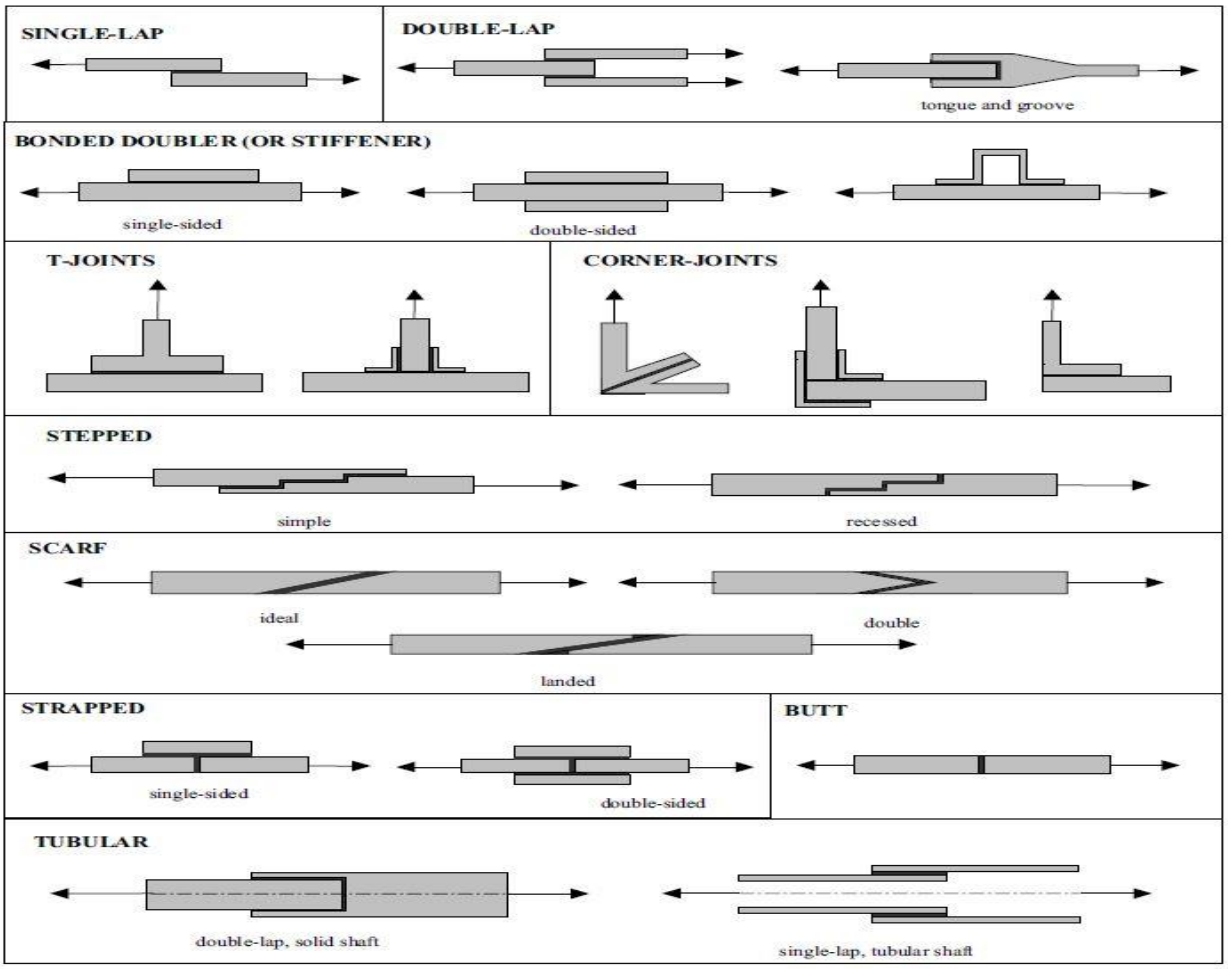

Fig. 4. Typical adhesive joint configuration [6]

Figure 4 demonstrates a portion of the typical bonded joint configurations. They are easy and cheap to fabricate and the shear lap joint is easy to examine ultrasonically because a complete inspection can be made from one side of the joint [2]. It is very important to comprehend the kinds of loading stresses associated with adhesively bonded joints. Strength of the glue joints predominantly relies upon the two major parameters; material accompanied by the glue joint and types of loading stresses involved within the joint. The fundamental types of loading stresses included in the glue joints are tension, compression, shear, cleavage as shown in Figure 5 [6].

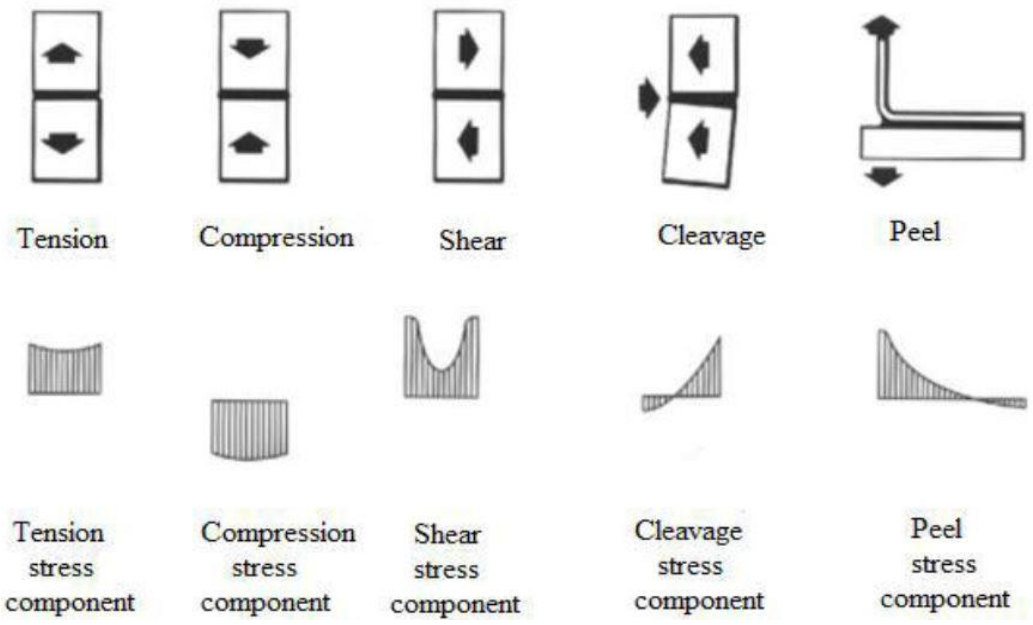

Fig. 5. Types of loading stresses in adhesive joint [6]

2.3. Curing effects of viscosity

The curing methodology demonstrates that any curing temperature increases lead to complete curing after a short duration until it achieves a level like a regime. The rate of reaction advances towards getting to be dissemination managed and the reaction is dropped. The testing was done for a month at normal temperature to complete the procedure and determine the properties of the samples. The aging test for 4h with 40°c in water vapor resulted that absorption of water acts as plastic behavior prompting conditioning of the glue. It has been exhibited that The tested samples were cured at various temperatures such as 23°c, 45°c, 64°c, and the factor of the conversion can be watched in figure 6. The temperature reliance of the curing was considered by DSC in figure 7 [5].

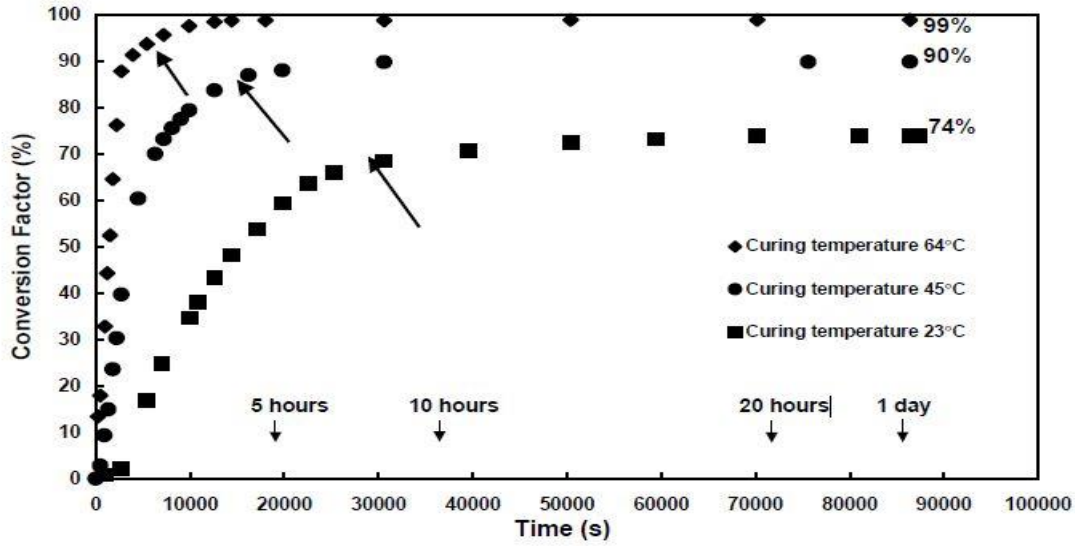

Fig. 6. Different temperatures of Curing Araldite [5]

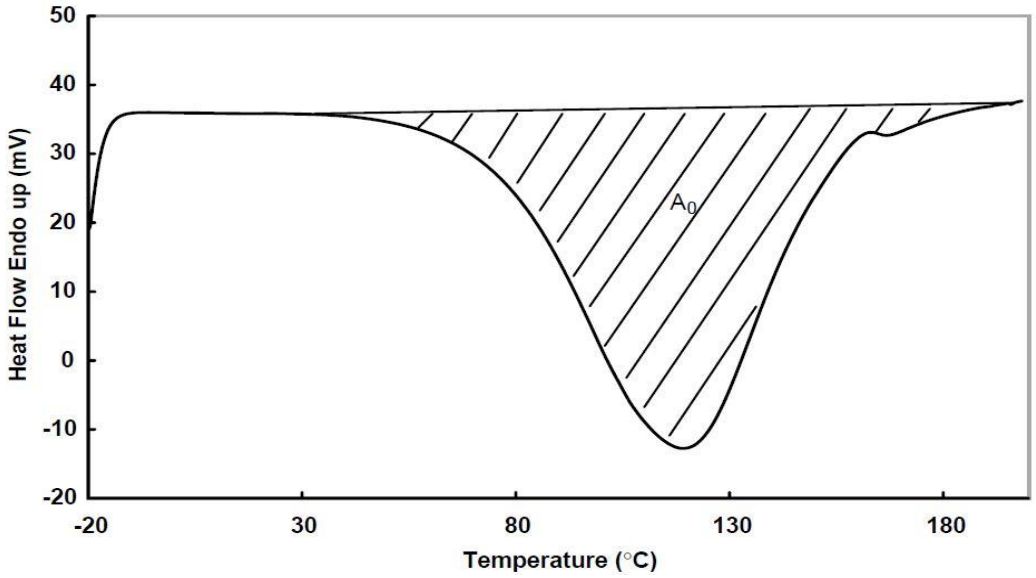

Fig. 7. Uncured samples [5]

2.4. Delamination and debonding failure

Due to poor interlaminar stresses failure present in the material which reflects the reduced strength, stiffness and prediction of materials durability. Delamination in composites can occur in two different ways which are delamination initiation and propagation. The energy discharge is assessed by VCCT. The delamination failure in model 587 of American airlines, where the fuselage was isolated which leads to ruin the control of the flight. The delamination elongates due to interlaminar stresses developed by the pressure difference of fuel. The analysis of delamination by theoretically and practically makes essential. An aircraft configuration to develop a list of material toughness on modern CFC, as of now being used for the fabrication of the frames in the aircraft [7].

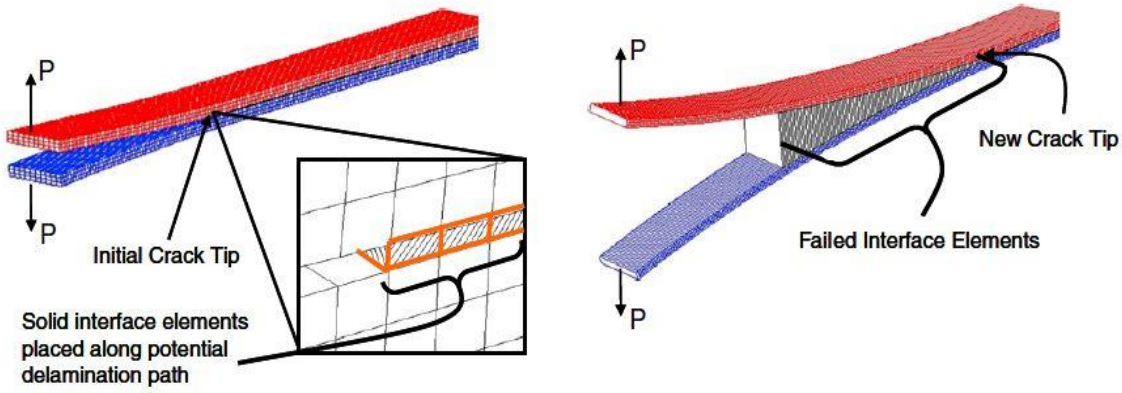

Fig. 8. Delamination‘s in double cantilever beam [8]

2.5. FE analysis

The ritz technique for numerical examination and simulation analysis for imprecise values was developed by R.Courant in 1943. Two kinds of investigations are mostly used in the industry 2-D

and 3-D Modeling. 2-D modeling for flat objects, it is simple and less time required to analysis but less accurate compared to 3D models. 3-D modeling, be that as it may, creates increasingly precise outcomes while yielding the capacity to keep running on everything except the quickest computers effectively. The Boeing company launched the FE method for analysis of stresses in aero-structures in the 1970s. The elements or nodes are been generated in the model for examination. The component‘s geometry is subjected to the kind of issue being examined. This helps in the reduction of time and expenditure and meshing elements can be introduced in high or low number to get precise values. The accuracy of analysis and computation resources are to be balanced for FEA. Among all other software, ABAQUS is familiar and used for solving engineering problems due to simplicity for complex linear and non-linear.[7].

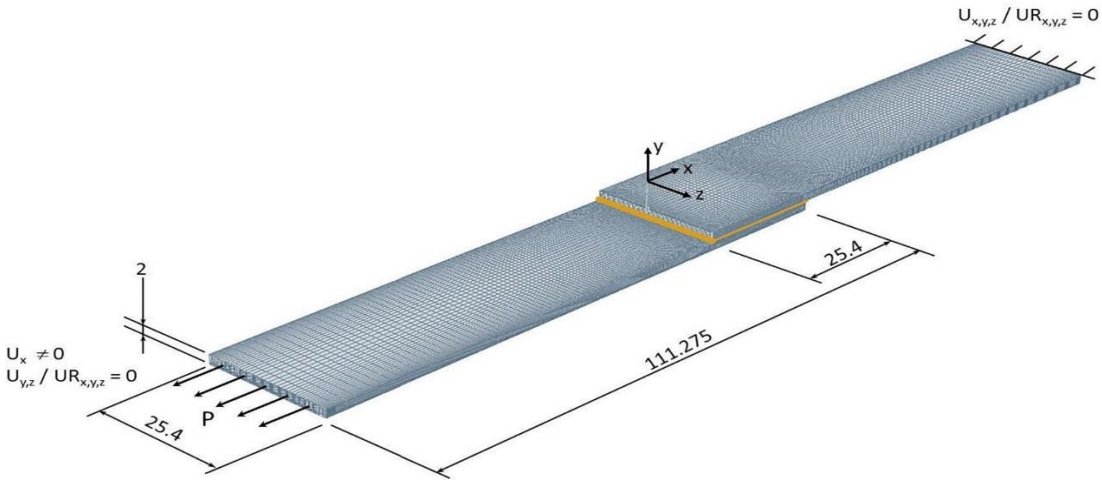

Fig. 9. FE analysis of shear lap joint [10]

2.6. Composite Wing spar

The spar is a structure of the wing structure that supports an aircraft on the ground and enables into a taxi, take-off, and landing. Present days, strength and weight of spar have turned into a significant factor. This part exhibits a way to deal with improve the structure of the spar of an unmanned aerial vehicle constructed using carbon fiber composite materials received from aerospace specification metals. First, the structural behavior is tested using the structural analysis when exposed to conduct limitations. The enhancement process is done iteratively to limit the thickness of spar which results in the minimum weight of spar [9]. The 0℃ lamina, orientation is impacted by the contact area of glue in composite causes failure and the 0℃ play orientation always prevents crack growth in the composite. From one viewpoint, the higher shear stress occurs inside of $[(0/-45/90/45)_2]_s$ laminates adhesive towards the adherends. Moreover, cohesive failure occurs inside the adhesive due to large peel stresses. In the composites, very large peel stresses happen in the glue when the presence of larger ply-angles. The specimen with 0℃ is failed in the bondline but small damage in the adherends. Figure 10(c) demonstrate that cohesive failure presence in the composites with yellow shades. The crack propagated (figure 10) up to the 3rd layer of the composite layup [10].

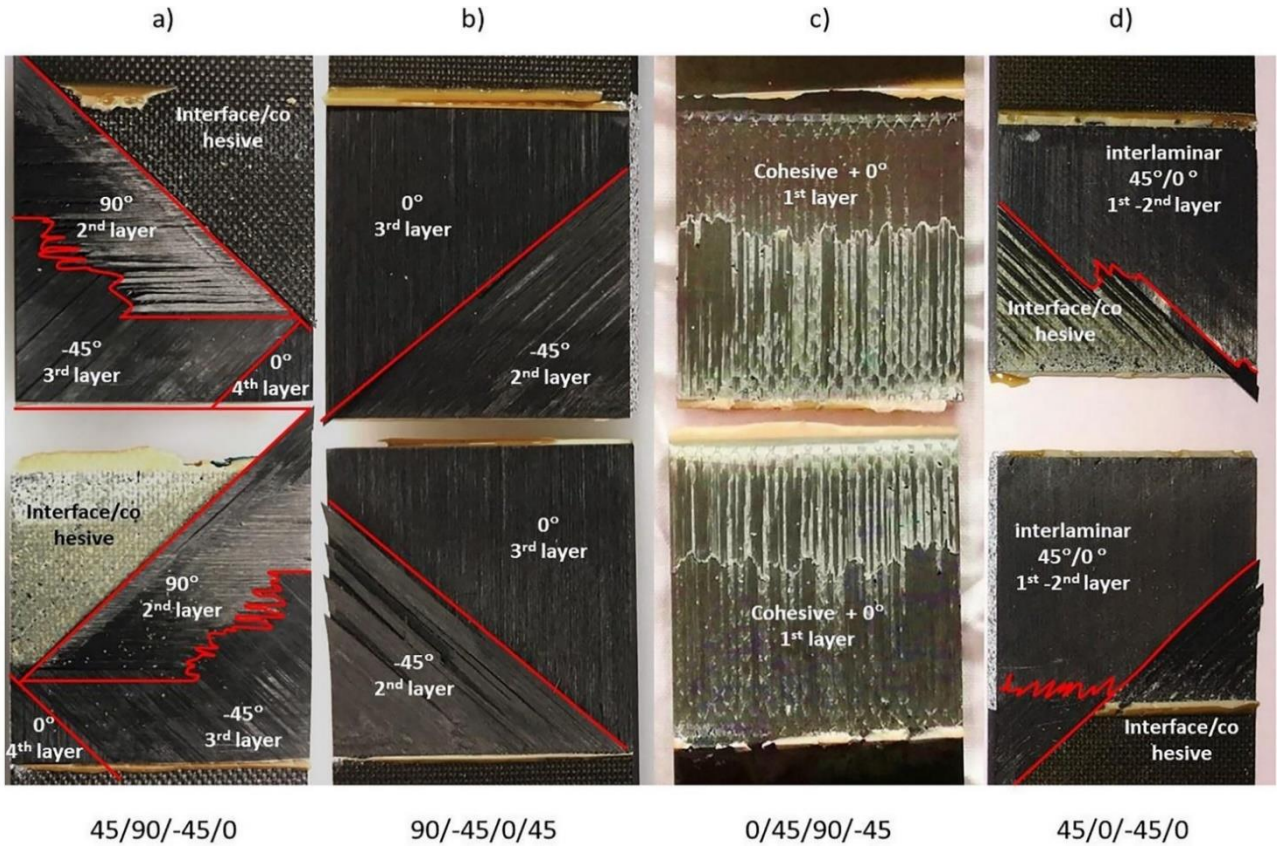

Fig. 10. Different types of failed surfaces [10]

Because of sweep and dihedral spar construction, considered to make the entire testing model of the spar that made to act load at the inner part as per the conditions required for testing environment.

The test was conducted on the fabricated part to remove the applying load at inner piece of spar which were created in 1-D, 2-D, 3-D. The element consists of 8 nodes with the required material, isotropic and elastic model. The core and walls were surrounded by carbon fiber to get orthotropic material nature of all laminated layers. To replace the phenomenon of contact, a rigid 1-D spar reflection was brought into use [27].

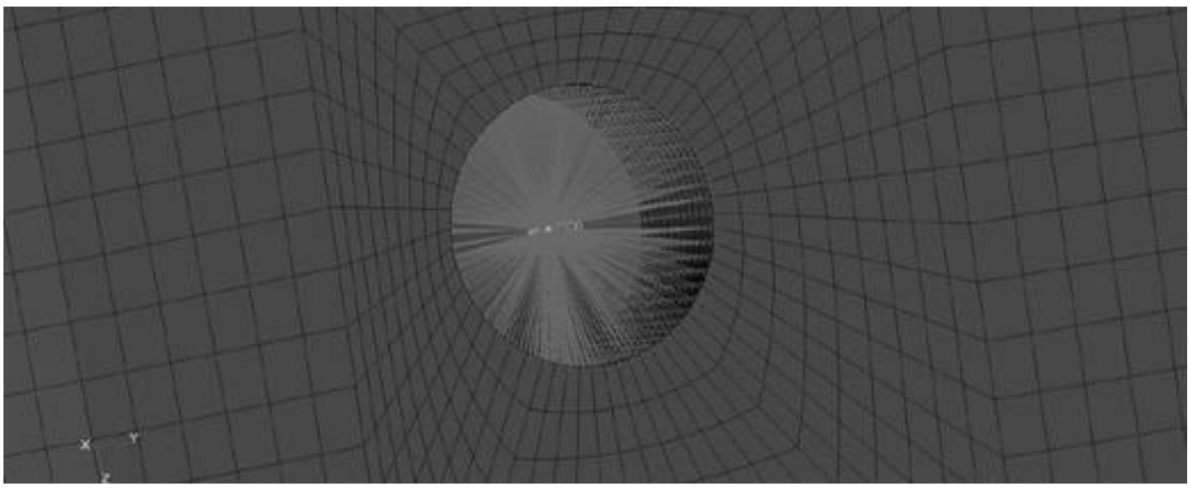

Fig. 11. Part of FEA mesh and 1-D elements simulating fittings

The plane bending was observed because of the resistance turning load in spars and also the chance of lateral movements in the lower and upper flanges of spars.

Fig. 12. Result of FEM analysis. Load factor n = 5.7 and−3.7 [27]

The care full examination was made each of 1000 load cycles, the displacement 0.01mm measures through ATOS [27].

2.7. Single lap and double lap joint

Theoretically, the most extreme glue stresses happen at point C and F in Figure 13. The stress difference exists at point A, F, D, C, because of geometry and material properties. The average stress occurs along the adhesive bond line. The Goland and Reissner models show that the normal stresses agree with theoretical expect constant stresses in the bond line [11].

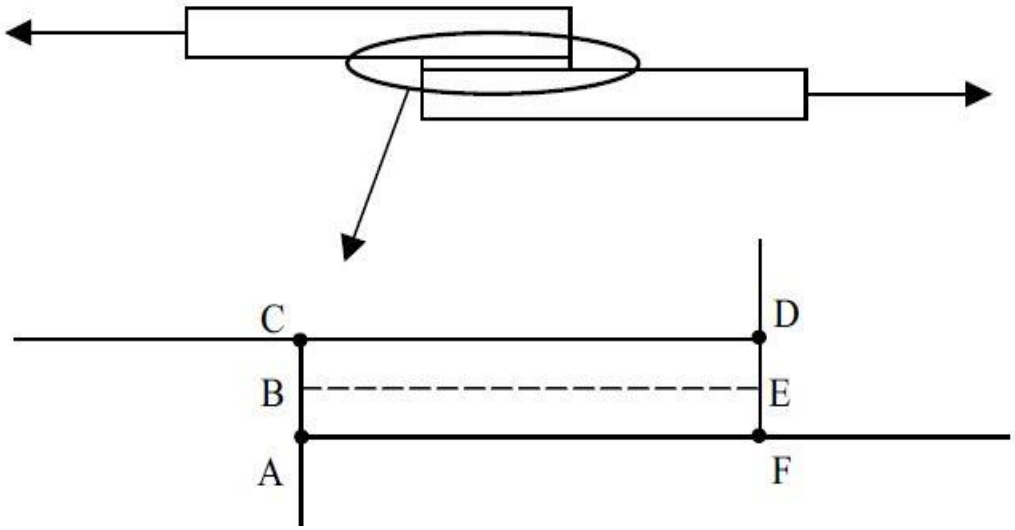

Fig. 13. The average stress location [11]

This shows the improvement and approval of a GBJM, an exceptionally proficient demonstrating system for catapulted composite joints. In the multi-bolt joints bolt-hole clearance, torque, friction between laminates can catch by using the GBJM. 3-D models single and multi-joints can be evaluated through GBJM and 97% of time-saving observed in FEMs [12].

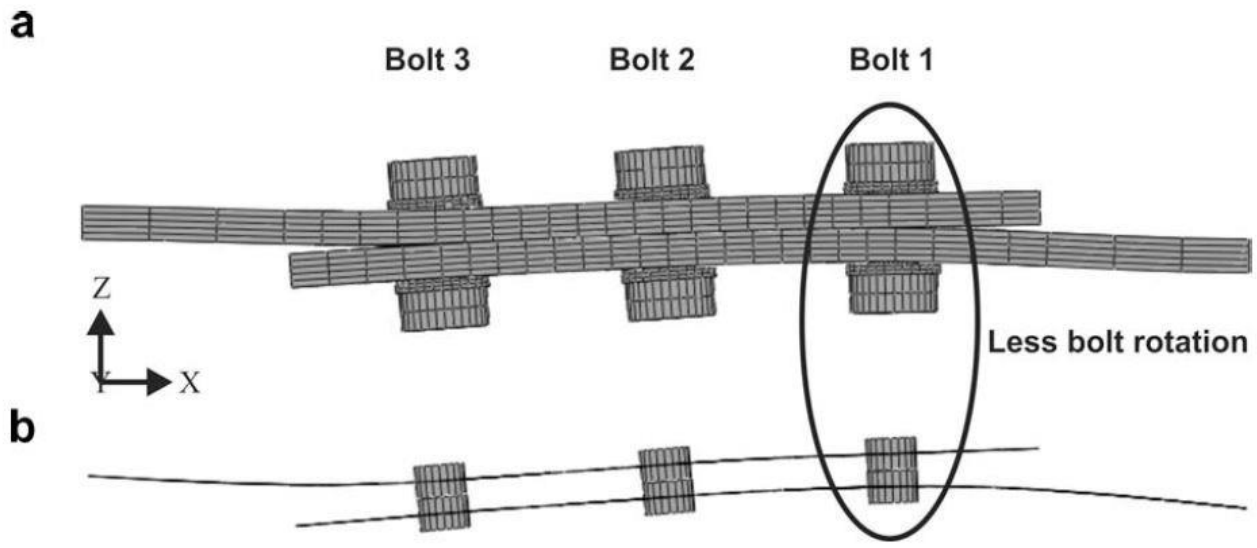

Fig. 14. Bending in a three-bolt, single-lap joint (a) 3-D FE model and (b) GBJM [12]

Figure 14 demonstrates that more clearance at the Bolt 1 than Bolt 2 &3, it shares most of the applied load. The multi-joint load distribution in composites shows the GBJM system and this system is suitable for the multi bolt and section joints. This methodology would lessen the requirement for practical analysis, reduction in cost for manufacture and test, proficient modification in aero components, subsequently featuring the quick modern industrials. The major aspect is for an assortment of investigation, the GBJM can estimate the failure due to the change of loading in stringer assembly and impact in real life situations[12].

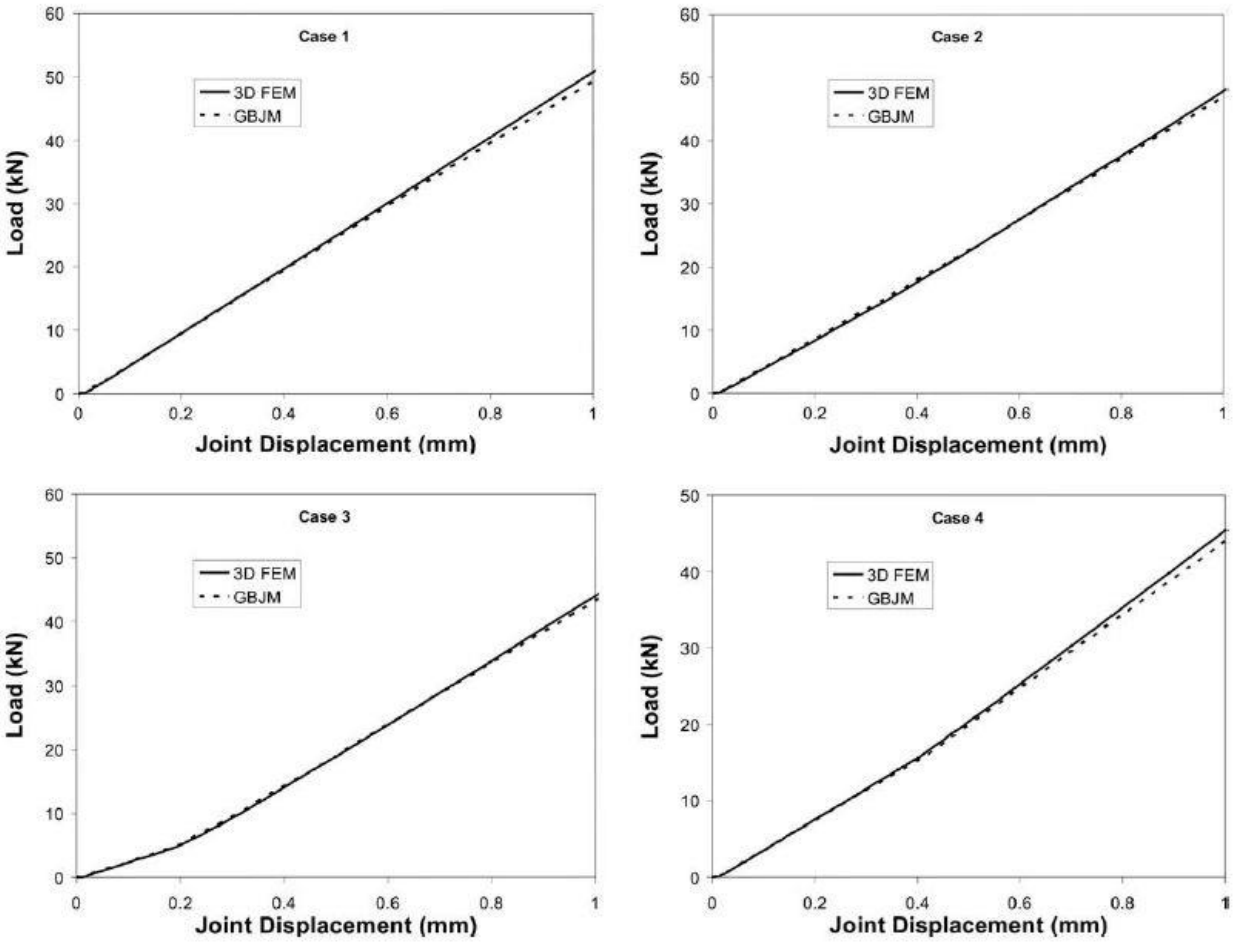

Fig. 15. Load-Displacement curves of different joints [12]

In figure 15 demonstrates the change of the (Single) bolt and lap joint resulting in 0.5 Nm bolt-torque, 10 micromillimeter clearance between the bolt and hole. The GBJM model where the deforms, secondary and tertiary bending at laminates, at the ends paddling is seen as of 3D model was observed quite well by both models figure 16 (b) [12].

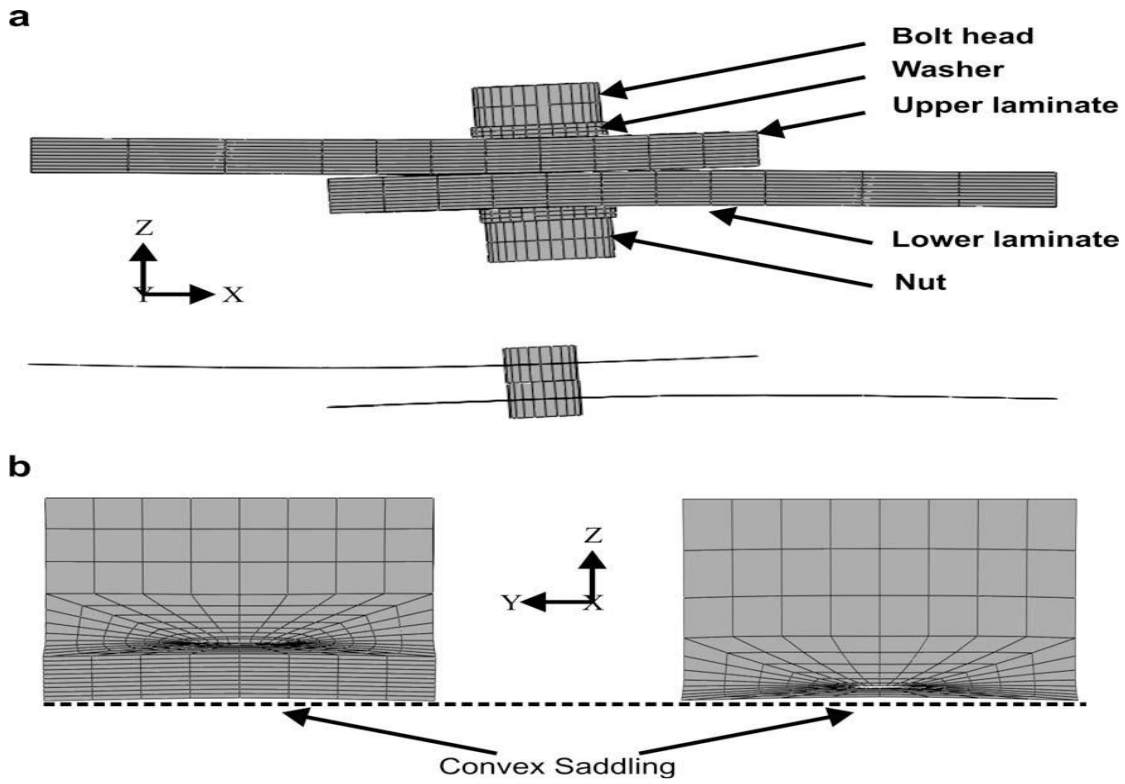

Fig. 16. Shear lap bolt joint in two views (a), (b) Secondary and tertiary bending [12].

The evaluation is carried for the improvement of the FE model for single lap joint by using lamb wave propagation and the ability to represent the model in the mathematical way easy for damage due to change in values of velocity discontinuity. By using Numerical simulations and experimental tests validated the proposed model [14].

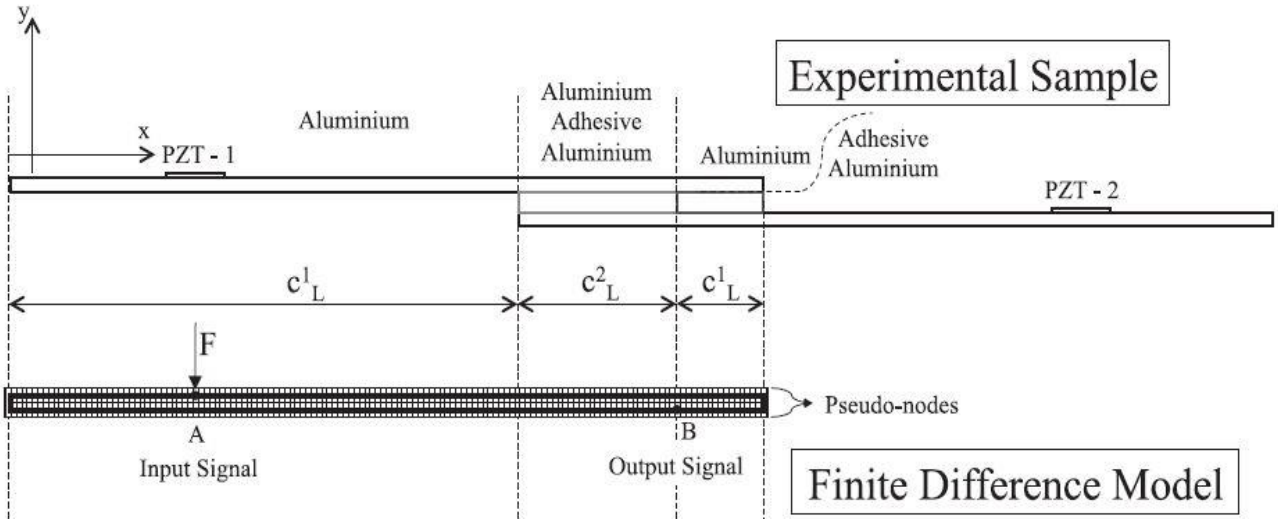

Fig. 17. Shear lap joint [14]

In spite of the productive viewpoints, they are liable deterioration at the layer of the bonds due to fatigue effect, disbands and vacuum found by inaccurate fabrication which leads to a failure by reducing the load carrying capacity. Due to these, the evolution of the SHM system becomes mandatory for safe adhesive linkage in complex construction. The SHM additionally makes the

superior learning of the behavior of the composition mechanically. After careful investigation of this joint was observed the damage with the signal content. Each frequency v_{att} was related with the signal which is generated and wave length observed experimental and nemerical outcome comes even for common geometry of the model. Due to the small symmetric property of the outcome across the linked region seen[14].

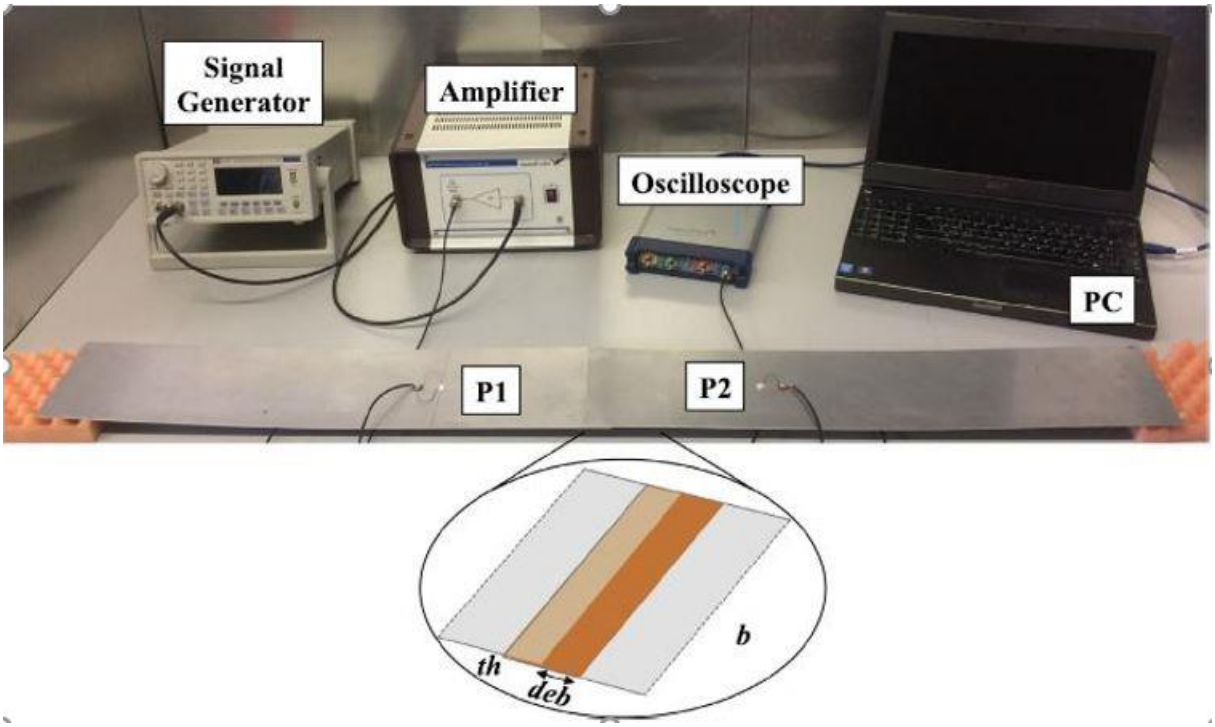

Fig. 18. Experimental setup of SHM single lap joint [14]

For estimating the bonding performance used the commercial software MSC Marc. Impact parameters such as cohesive thickness, length, stress distribution, debonding between the cohesive and aluminum plate. In this work, the implementation of cohesive zone model in marc is based on two types which are Interface elements and New material model to characterize the Interface behavior. We consider the individual properties of the matrix material and cohesive separately [15].

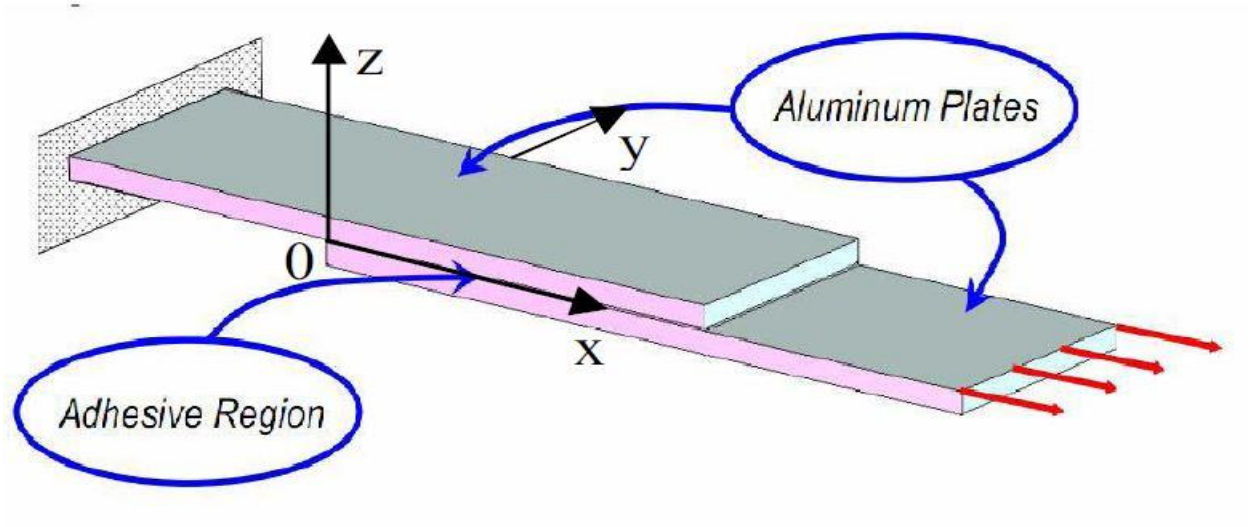

Fig. 19. Shear lap joint [15]

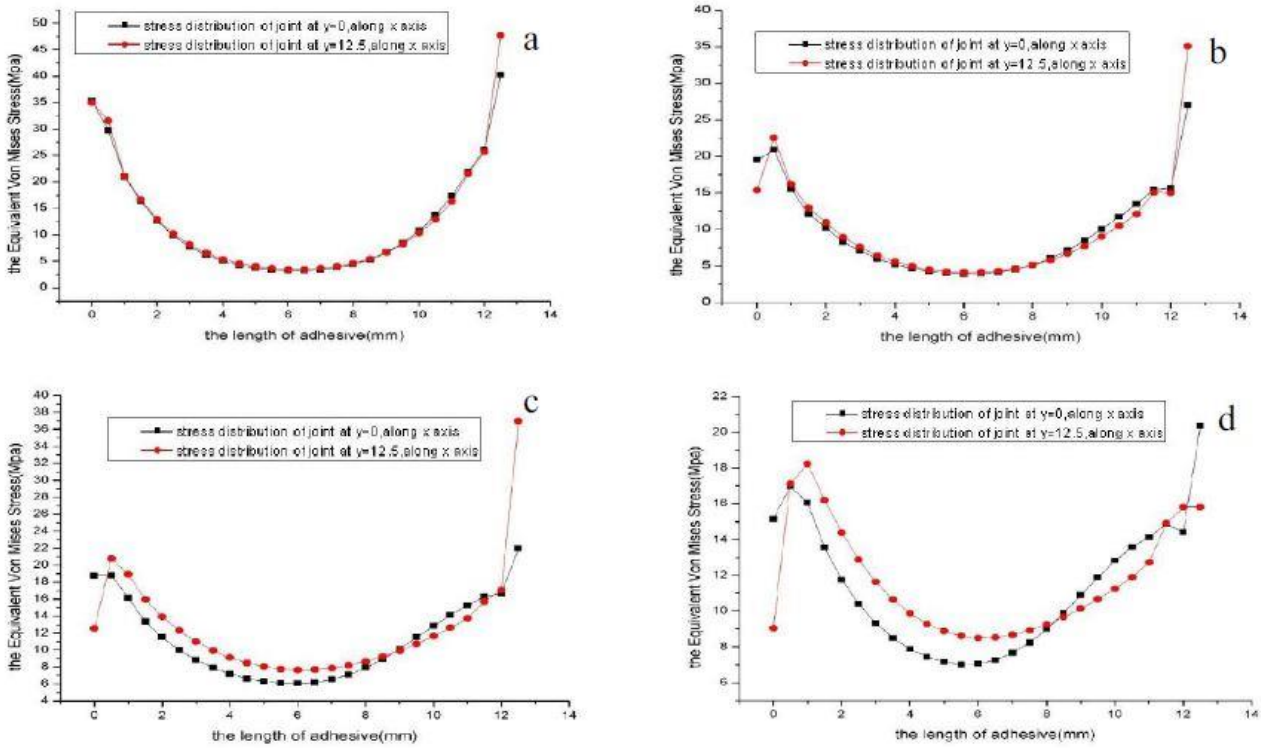

Fig. 20. Stress distribution varies with the thickness of adhesive [15]

Above figures show that equivalent Von Mises Stress of adhesively bonded joints with an adhesive thickness of 0.1mm Figure 20 for 0.2 millimeters, 0.4 millimeters, 0.6 millimeters respectively (for a, b, c, d), the length of joint of adhesive 12.5mm. Under the same load, the Equivalent Von Misses Stress in the connection varies with the thickness of the material used for bonding at a different location could be seen. At the same load, the hump of the stress in the adhesive joints varies from 40.23 Mpa to 27.04 MPa, 21.98 MPa, and 20.35 MPa at y=0, along the x-axis. Stress in the adhesive joints is 47.7 MPa, 35.05 MPa, 36.95 MPa, individual at y=12.5mm, along y-axis showing in above figure 18. At both locations, stresses in the joint descend gradually with an increment of

adhesive thickness [15]. The mostly stress analysis is done on balance joint that is established by de Bruyne in 1944 Volkersen-de-Bruyne arrangement created utilizing Volkersen's hypothesis (single lap). The shear stress and lag methodology obtained upon modeling the bars which are not deform due to shear are made by adherends. The glue in the connection acts as a shear spring conveying the stresses by shear need longitudinal force in the adherends from the inner portion to the outer. Afterward, Thai-et-al in the year of 1998 had provided with proven performance that includes tear deformation in the product. To predict, the technique which is for the parameters of double stress singular is taken into account for the growth of the fatigue tendency. The concentration of the stress can be lowered at the surfaces of the piles and at the edges of doublers[26].

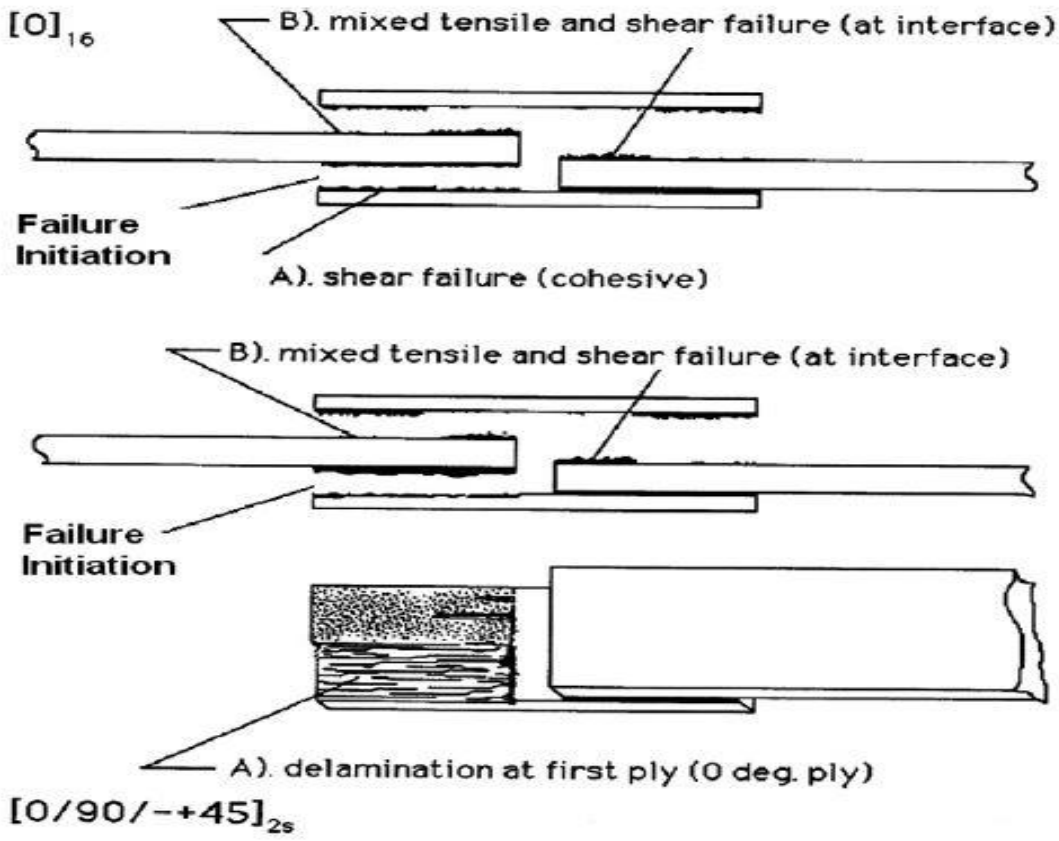

Fig. 21.Due to tensile loads delamination in unidirection and quasi-isotropic specimen of double lap joint.[26].

From the experimental, numerical and theoretical results derived the pressure distribution, two-sided connections within single direction and quasi-isotropic of sandwiched composites mechanics. As per experimental and FEM results are good for analysis of displacement. Compressive deformation occurs cross-section close to end and elongation occurs in the same direction as compressive deformation but it‘s close to the furthest limit of the adherend [26].

2.8. Cohesive Zone Modelling

The conventional techniques to predict the strength of linked joint such as continuum mechanics or LEFM-based is a proven technique in the last 10 years, but its limitation to minor yield ahead of the edge of the crack. The CZM has been introducing around 1950 or beginning of the 1960s by

Barenblatt (1959), Dugdale (1960) for static applications. CZM is based on spring or more typically cohesive elements, the solid element of connecting two-dimensional, three-dimensional assemblies. The CZM laws can be effectively incorporated in conventional FEM software to simulate crack propagation in different materials, including sticked connections. The establishment of this method because of laws of cohesion between the inner surfaces or minute regions [16].

Many investigations were carried out through practical and 3D explicit FEMs at different types of overlap lengths of shear lap adhesive bond. The nature of the failure is different in each overlap lengths. Every norm is customized by the utilizer explicit valves using node detection. The models disregarding interface components can't simulate the delamination at the point due to the models under cohesive, acquired to know the cause of damage. From cohesive zone models impact of the removal of sandwiching, broke down thoroughly to recognize this issue. Investigation on load acting upon the connected distance of 10 mm shows the maximum effect at glue connection along the axis [29].

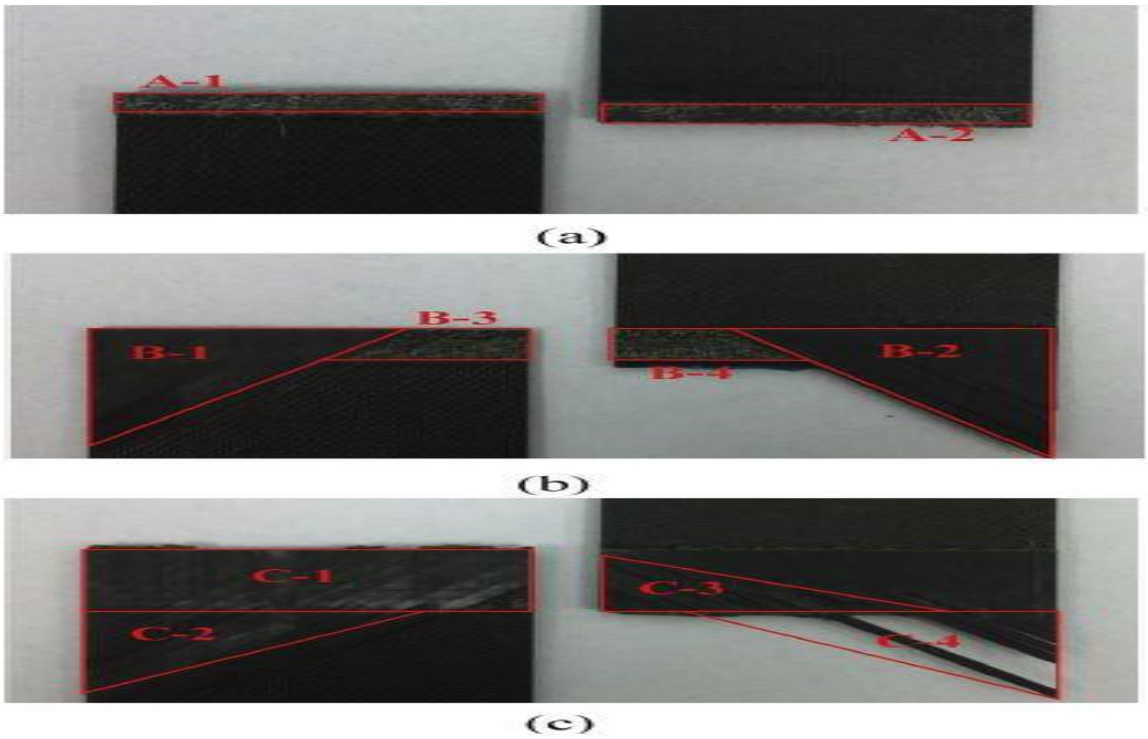

Fig. 22. Failure modes at the various overlap of adhesive lap [29]

Figure 22 demonstrates that the sticker link as safe for all above assemblies, of cover across the 10mm. The delamination occurs at the overlap area in both model I and model II and delamination propagate along the direction of the fiber. In the 1st and 3rd models seen that as matrix damage and fiber damage, it's basically steady with the tensile and a fraction of the fiber for the C3, C4. But the 2nd model is stopped from elongation at the connection [29].

In particular the mode of defect is for the 50 mm which is a failure due to glue for the 100 mm overlap, generally, glue, a region of defect likewise watched. For predominant failure, modes have seen by as larger over-lap between 150 to 200 mm because of fibers remove separately [30].

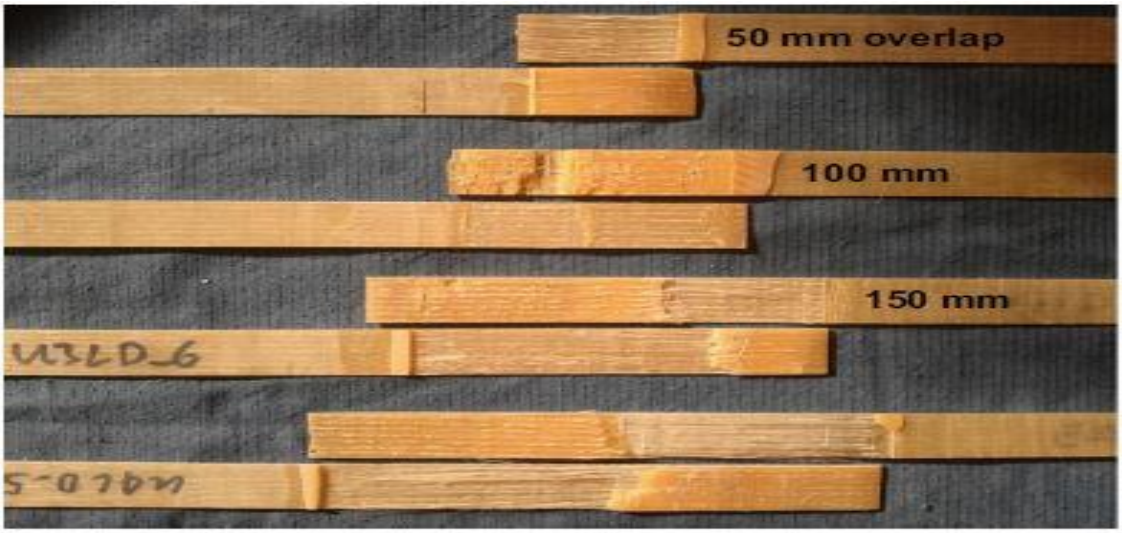

Fig. 23. Various types of adhesive joints [30]

By comparing FE results and test results observed the strength of the overlap of the joints. The length of the lap joint is 150mm to approach their maximum strength observed in the tests and FE results. The most distribution of load is at the overlap corners during the un-bonding process which tends to separate the connection[30].

Table 1. adhesive bonds failure loads [30]

Bonding due to secondary				Co bonding			Reference	
Overlap Length mm	Finite Element Analysis in kN	Test conducted in kN	COV in (%)	Finite Element Analysis in kN	Test conducted in kN	COV in (%)	Test conducted in kN	COV in (%)
50	10.27	6.64	22.10	15.60	11.61	9.70	24.88	3.10
100	13.62	10.51	8.80	16.36	16.36	9.23		
150	14.10	14.83	4.67	16.74	16.74	7.63		
200	14.11	14.65	4.20	16.60	16.33	3.28		

2.9. Lap joints in aircraft

The two different configurations of lap joint used in aircraft tested under static load are aluminum alloy 2023-T3 and carbon fiber reinforced epoxy doublers with same adherends and different adherends, riveted connection, bond or hybrid connection between surfaces and different composites [31].

Fig. 24. Adhesive failure with AA2024-T3(left) and mixed CFR bonded connections(right) [31]

Fig. 25. Hybrid joint failure with AA2024-T3(left) and mixed CFRE(right) [31]

Experimentally and numerically proved that adhesive bonding is 5 times stronger than rivet connections, others are found to be better, due to high stiffness. One more thing is that metal to the metal joint has a 70% higher strength than hybrid metal to composite joints. The Hybrid joints of metal doublers with rivet and adhesive joints were found to be a failure and their is 2% variation in practical as well as calculated values of load vs displacement curves. The metals with the composites doublers of stress intensity factors are tested with the length of the cracks are 15mm and 10mm under riveted and bonded configuration [31].

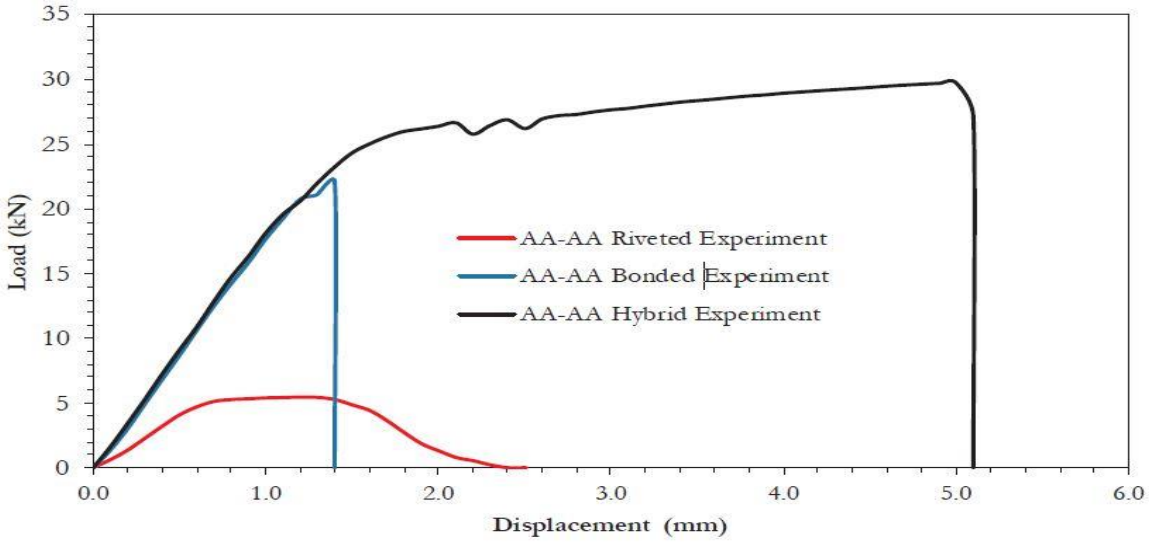

Fig. 26. Load-displacement plot as per adhesive bonds and riveted and hybrid joints with AA2024-T3 [31]

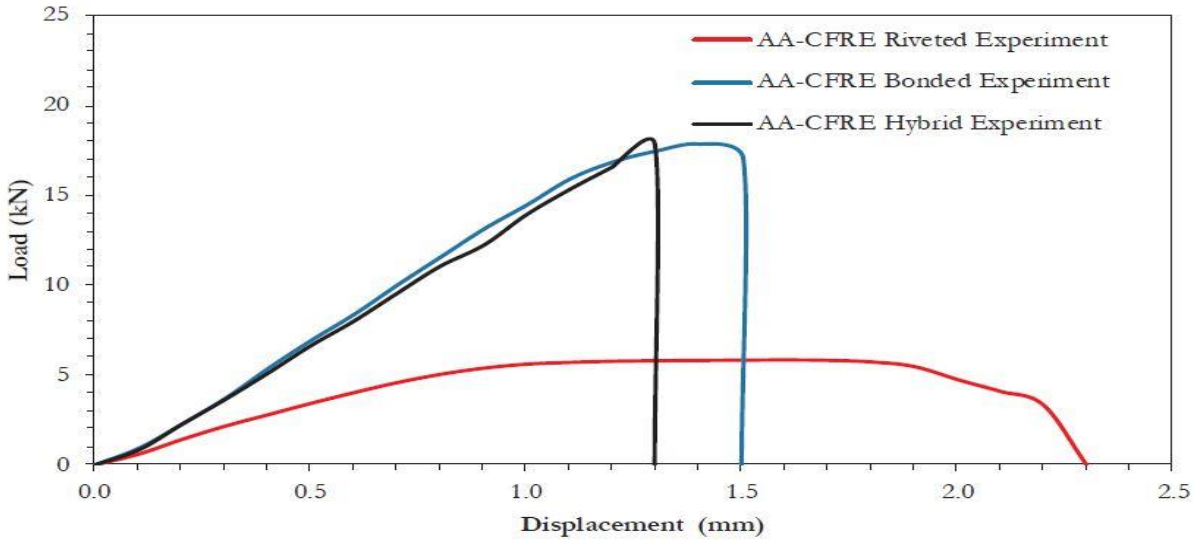

Fig. 27. Adhesive bonds and riveted and hybrid joints with CFRE load vs displacement curve [31]

Single overlap built by aluminum with carbon-fiber connections tried for the good conduct of nonsimilar joint. By using the method of correlating imaging digitally observed for local deformation within specimens. In ABAQUS the access to Cohesive zone modeling which can do the simulation on the behavior of yielding due to tearing in overlapping glue connections. Examinations demonstrate that the utilization of divergent Al-C and C-C connections causes the decrease in the bond strength and lower the stiffness within sandwiching and breaking of carbon-fibers. The numerical solutions overrate the practical yield-strength and nonelasticity or inflexibility in the connections [32].

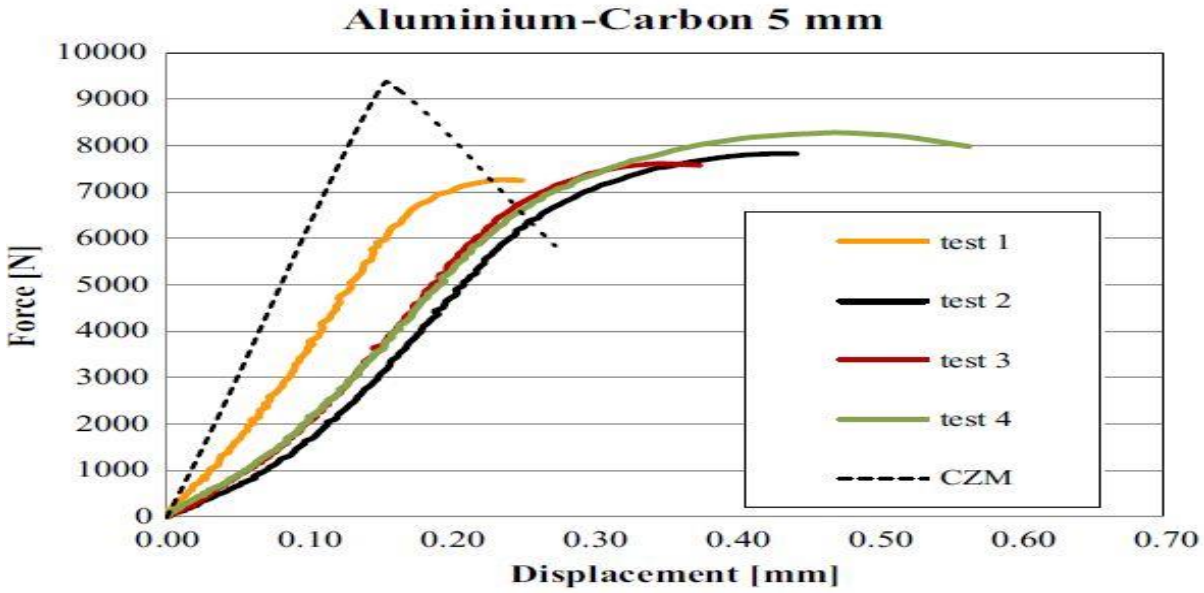

Fig. 28. Plot for F-D curves from numerical and practically for Al-carbon bond [32]

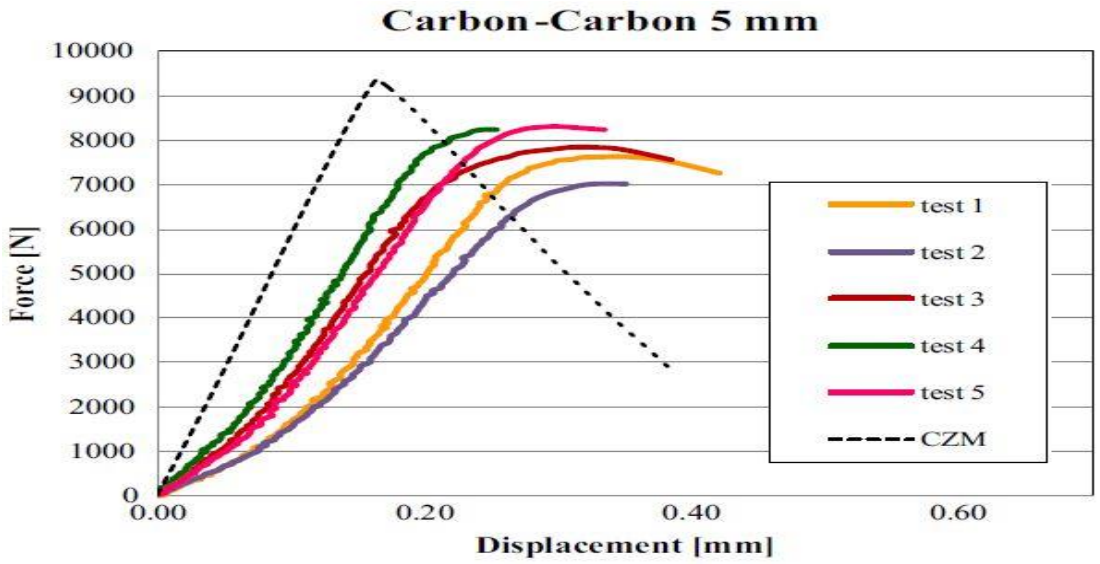

Fig. 29. F-D curves from numerical and Practically for carbon-carbon joint [32]

Aircraft structures looking for light-weight and strong structures. The investigated on the reduction of I-cross section of an inner wing constructed of aluminum 2024-T3. By using of finite method observed fatigue life and XFM ability to perform the crack growth even in complex geometry. The calculation was completed in Morfeo or crack of software ABAQUS programming based upon the execution XFEM software. The crack formation of different shapes and fixed cross sections area were compared to know better among them[33].

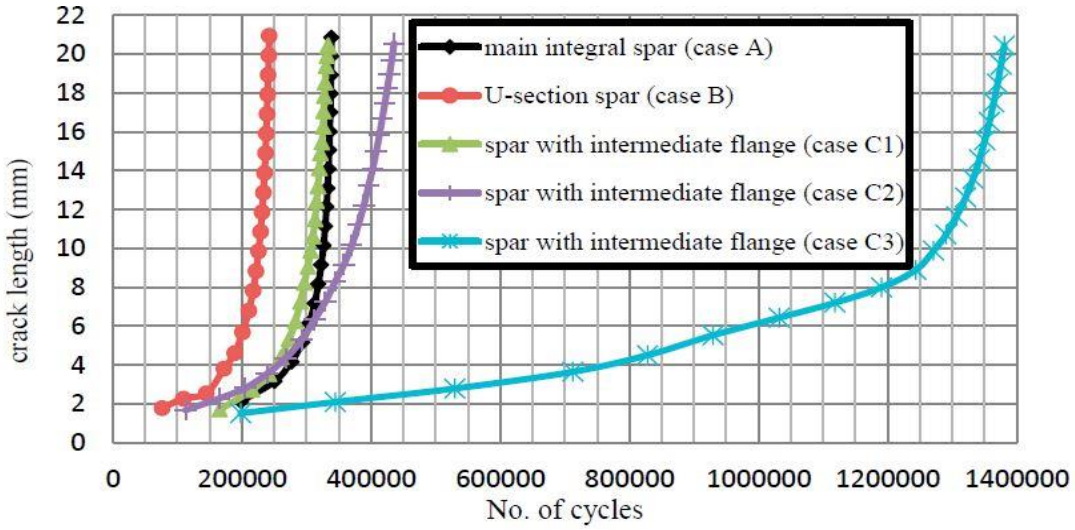

Fig. 30.The comparison fatigue life of various cases [33]

In figure demonstrate that the life-cycle under fatigue for C3 for a number of cycles at a=21mm which are than 1,000,000 cycles more than in case of A. For C2 an increment from 100 mm to150mm and C3 had a bigger Inertia of moment and small displacement about 2.705mm [33].

Table 2. Displacement and moment of inertia of different types of spars [33]

Model	No.	Cases	I in mm^4	Displacement (mm)
Integral spar	1	A	654.0	3.0
U- shaped spar	2	B	558.0	3.5
I-Shaped spar	3	C_1	583.0	3.3
	4	C_2	662.0	2.9
	5	C_3	726.3	2.7

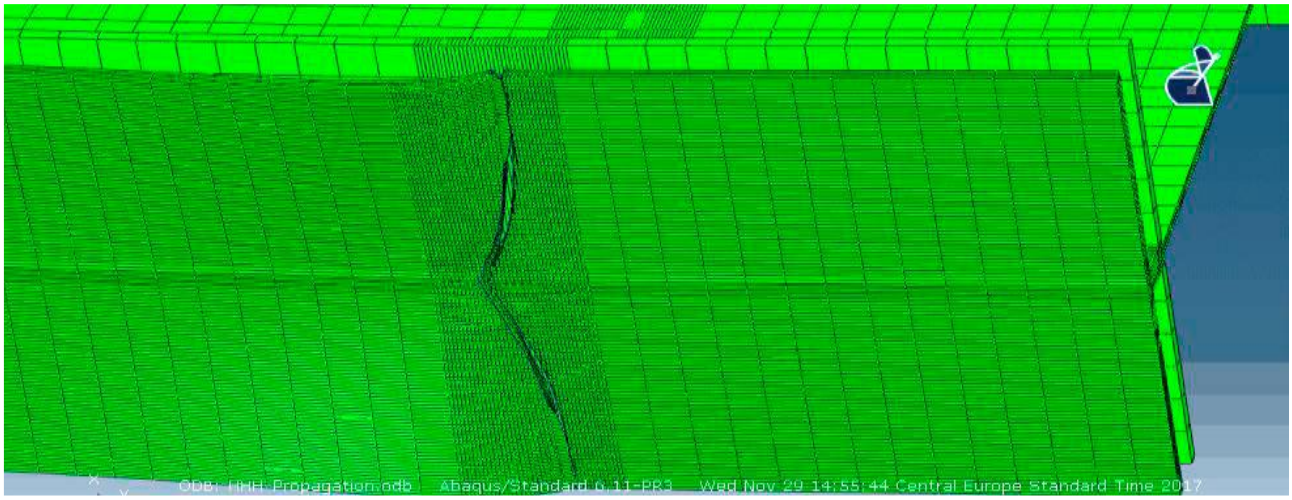

Fig. 31. Cracks on bottom cap (C2) [33]

3. SINGLE LAP JOINT ANALYSIS

3.1. Carbon fiber

Carbon fibers are of high strength and light material. That is currently used as a part of high esteem products where high strength-to-weight proportion and unbending nature are required, for example in, aviation, car, structural building, and games merchandise application. Carbon filaments also have high rigidity, high ductile modulus and compressive quality [4].

3.2. Adhesive bonding

A large fraction of modern glues are carbon-based petrochemical derivatives. The basic holding procedure can be surface absorption (intermolecular or inter-atomic fascination powers amongst surface and cement), synthetic holding (van-der-Waals powers, valence bonds), dispersion (interfusion of glue into the structure of polymeric bond accomplices), electrostatic fascination and mechanical interlocking [4].

3.3. Mertis of adhesive bonding

- The ability or capacity of bonding different materials.
- The easy and Inexpensive joining system.
- Sealing properties (glue fills holes and all the voids).
- Joints must be electrically and thermally insulated
- It eliminates galvanic erosion
- It provides good vibration damping properties
- Uniform distribution of mechanical stress over the joint
- Offer good fatigue resistance

3.4. Demetris of adhesive bonding

- The cautious is to be taken for substrate (follower) surface planning
- Duration for blending and curing might be required comparatively more.
- Difficulty in the dismantling of parts once connected.
- The apparatus required to stabled (held in position) the joined parts amid curing
- The service temperature and condition are maintained.
- Low creep strength is observed.
- The properties vary during service or usage.

3.5. Adhesive bonding stages

1. Assembly and joint design: Legitimate plan gives negligible peel and cleavage stresses. Tension, compression and shear stresses may be increased.
2. Adhesive selection: Determination of appropriate cement depends on the substrate material, temperature condition, prerequisites to the holding quantity, adaptability and strength.
3. Surface preparation: The substrate surfaces ought to be cleaned from soil and oils, and then scraped. Perfect and roughened surfaces give great wetting of the glue, which brings about solid grip.

4. Applying and spreading a proper amount of the selected adhesive over the substrate surface: The task is performed either physically or by methods for apportioning gadgets.
5. Gathering of the parts to be joined.
6. The operation is performed either manually or by means of dispensing devices.
7. Assembly of the parts to be joined.
8. Clamping the parts in a fixture at a controlled pressure.
9. Curing: Curing processed by heating or radiation [4].

3.6. Experimental results

INSTRON E10000 electromechanical test machine was used for performing the analysis of carbon fiber bar single lap joints. The cross-section of the bars is square (3.2 x 3.2 mm). The working length of the unilateral sample shown in figure 32 was 20mm. The long chain type specimens were placed in the square tubes containing polyethylene inserts. The shear lap joints are fixed directly with the machine edge grips. During the approval, the difference between the direction of the force and the axis of the test piece was not more than ± 0.5 °. The examples after consolidation were kept up at a temperature of 80 °C in a thermostatic domain for 3 hours. The residual strength was measured for carbon fiber bar specimens (figure 32) bonded with UN-3082 epoxy film adhesive with uniform tensile load(1071, 391, 1151.33, 1437.33 N) applied the help of Instron series IX software for controlling the test machine [4].

Table 3. Stress and strain curve fitting table [4]

	P_1	P_2	R-square
1	5849(5841, 5858)	3.83(3.637, 4.022)	0.996
2	8034(0.1574, 0.2194)	0.1884(0.1574, 0.2194)	0.998
3	1.813e+04(1.401e+07, 1.417e+07)	5.387(5.256, 5.514)	0.992
4	1.409e+07(1.401e+07, 1.417e+07)	7.056e+07(7.017e+07, 7.095e+07)	0.999

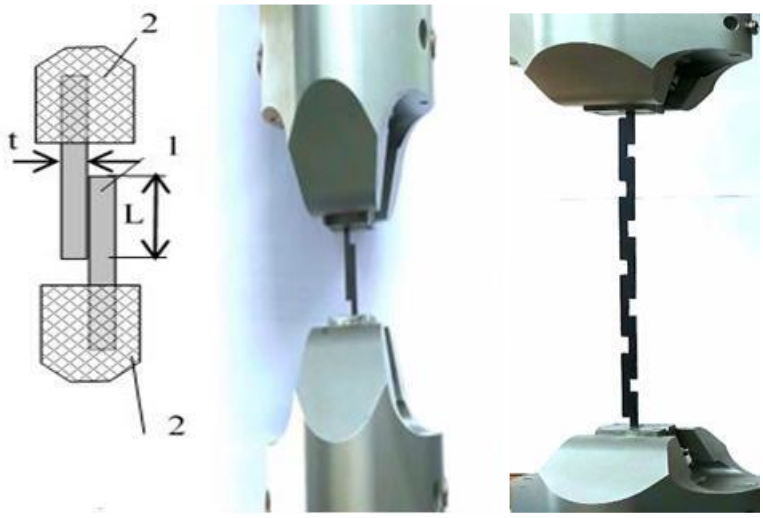

Fig. 32. Static test of the specimens [4]

The regression formula for shear stress and linear strain relationship

$$\tau = P_1 + P_2\varepsilon \tag{1}$$

where τ is the shear stress, ε linear strain.

Practical results of the specimens are presented here and coefficient of variation, median, standard deviation, mean, minimum load and a maximum load of four specimens are calculated. Therefore, these parameters (ultimate force, stress, strain at breaking point) are dependent on the adhesion properties. Figure 33(a) shows the load and extension of the four different loads on the specimens after the ultimate strength. There is sudden extension or peel of the joint is noticeable in figure 33(b) [4].

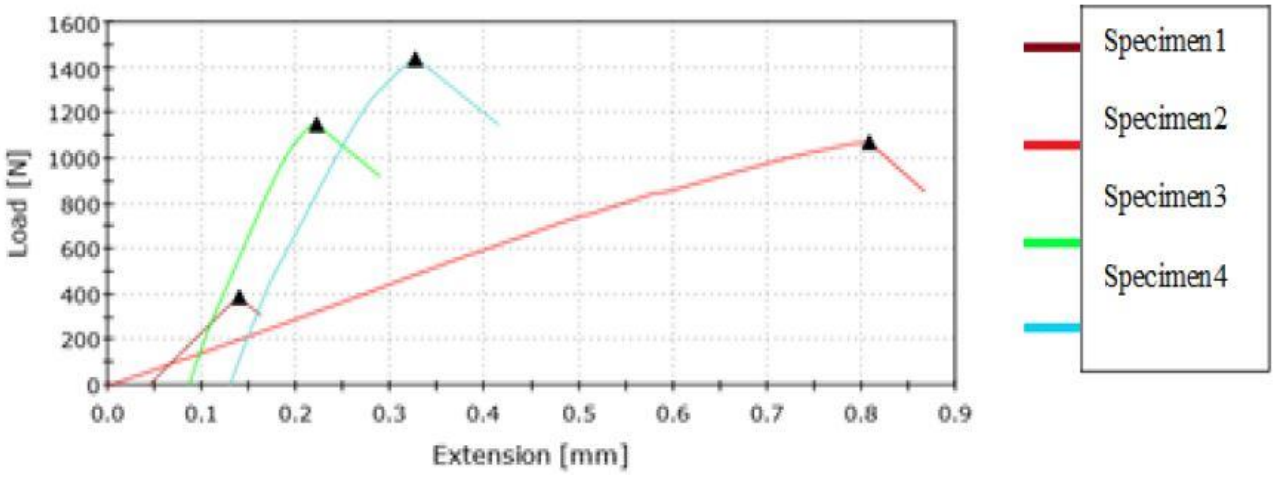

(a)

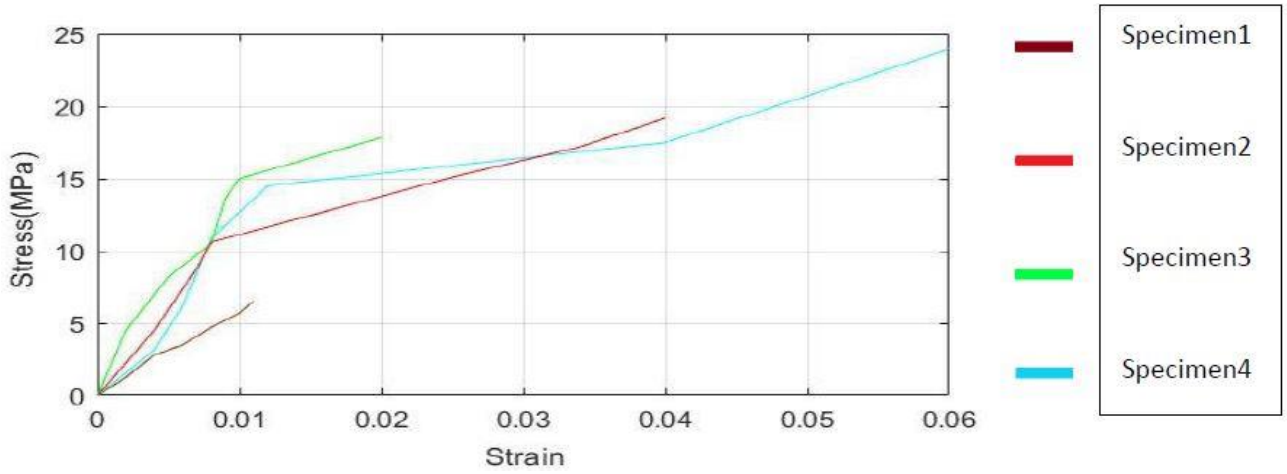

(b)

Fig. 33. static test diagram of the specimens [4]

3.7. Numerical analysis

Important theories of glue joints are adsorption, mechanical, electrostatic, diffusion joint weaknesses and the theory of adsorption stresses the way that when glue and glue materials are in contact, the traction forces occurs, and this studies about the adhesive strength. Diffusion theory provides information about the polymer adhesion model and explains the dependence of adhesion on time and molecular weight. The essence of the weak layer of the connection consists of determining the adhesive weakness and assessing the state. Using formula 2 the average tangential tension area was calculated which was in contact(overlap), 16.73MPa, 6.10 MPa, 17.98 MPa, 22.45MPa with loads 1071, 391, 1151.33, 1437.33 N respectively.

The average tangential tension in the contact area can be calculated as [4].

$$\tau = \frac{P}{BL} \tag{2}$$

Where F is a force, B is the width of the bar, L is the length of the contact area. Distribution of tangential and normal stresses in the zone is uneven. Strength of the materials approaches typically suggest that when certain stress components or an equivalent stress component (e.g, Con Mises equivalent stress), suppresses its allowable counterpart dependent on the material property, failure will occur. The most important components of the adhesives are shear and peel stress. The shear distribution τ and the peel stress σ in the adhesive along the bond line are given by

$$\frac{\boldsymbol{\tau}}{\boldsymbol{\tau_{av}}} = \frac{1}{4+3\zeta}\left[(1+3k)\ \frac{\delta}{\sinh\delta} cosh\left(\frac{\delta_x}{c}\right) + 3\ (1-k+\ \zeta\ )\right] \tag{3}$$

and

$$\frac{\sigma}{\sigma_{av}} = \left(\frac{t}{c}\right)^2 \frac{1}{\Delta}\left[\left(\frac{r_1\lambda^2 k}{2}\right) k'\lambda\ \sinh\lambda\ \sin\lambda)\ \sinh\left(\frac{\lambda_x}{c}\right)\sin\left(\frac{\lambda_x}{c}\right) + \left(\frac{r_2\lambda^2 k}{2}\ k'\lambda\cosh\lambda\ \cos\lambda\right) cosh\left(\frac{\lambda_x}{c}\right)\ cos\left(\frac{\lambda_x}{c}\right)\right] \tag{4}$$

where τ is the adhesive shear stress, τ_{av} is the average adhesive shear stress and Δ is constant, ζ is the ratio of adhesive to adherend thickness, C is the half of the overlap length, t is the adherent thickness, σ adhesive peel stress, σ_{av} is the average adhesive peel stress, k and k' are the constants of linear related to the applied load [4].

3.8. Observations

The image of carbon fiber rod connections after fractures is shown in figure 34. It can be noted that the nature of the decay may be different. The irritation in the adhesive is shown clearly. On some occasions, decay occurs inside the carbon fiber rod [4].

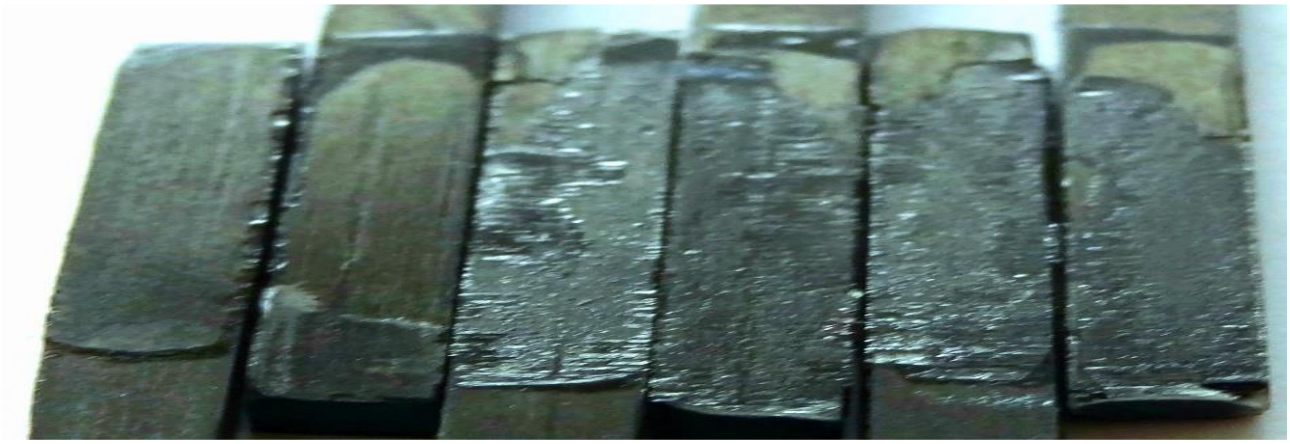

Fig. 34. Lap joint specimens after fracture [4]

The above figure demonstrates the adhesive peel stress and shear stress occurs during the experiment. Because of the pressure peculiarity, large stresses occur at the joint corners. The disfigurement and prolongation happen when the load increments keeping on mind the end goal to watch the shear stress, peel stress are dependent on the glue thickness and material properties. We have observed the ultimate forces and stress with the specimen and it‘s deformation point with respect to change in adhesive thickness and material properties change. Different outcomes are obtained along with distinctive deformation. Glue viscosity and overlap of the specimen increments incomes about the loss of deformation percentage. By the experimental and numerical analysis calculations, the average shear stress distribution is the almost same. Most accurate forecast of the break-down moments is obtained. The durability of such joints can be predicted by deformation measurements.

The figure 35 (a, b) shows the adhesive bonding of the carbon fiber rod that is bonded together for a certain amount of stress and started deforming and peeling from the joint after its ultimate strength is visible [4].

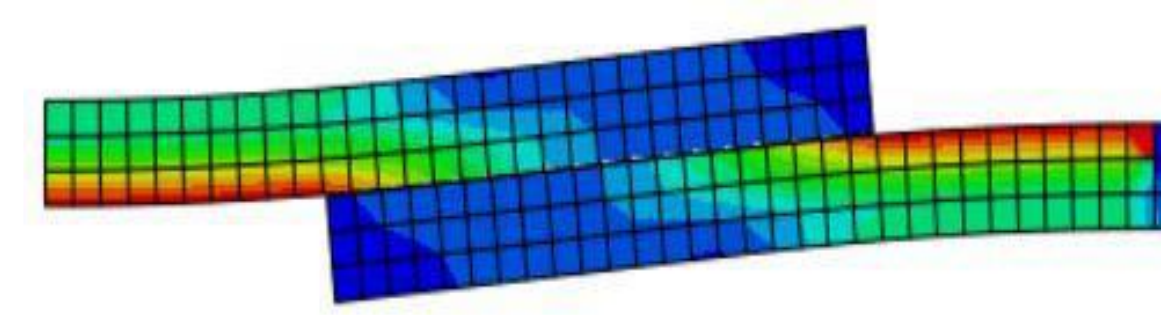

(a)

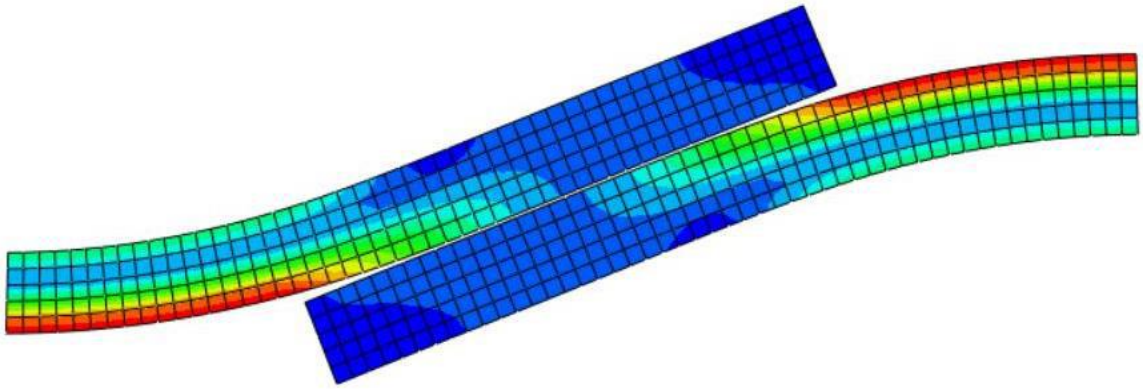

(b)

Fig. 35. The deformation of single lap joint at different loads (a) no crack (b) cracked and overlap [4]

Figures 36 illustrate the shear stress distribution along with the adhesive bond and perpendicular to the adhesive bonding. The marked lines demonstrate the stress distribution at various loads, which is related to the displacement of the upper clamp. The maximum displacement of the upper clamp is v=0.5 mm. Unmarked lines show the shear stress distribution of two nodes, which are located closely one to another on joining bars during the load process [4].

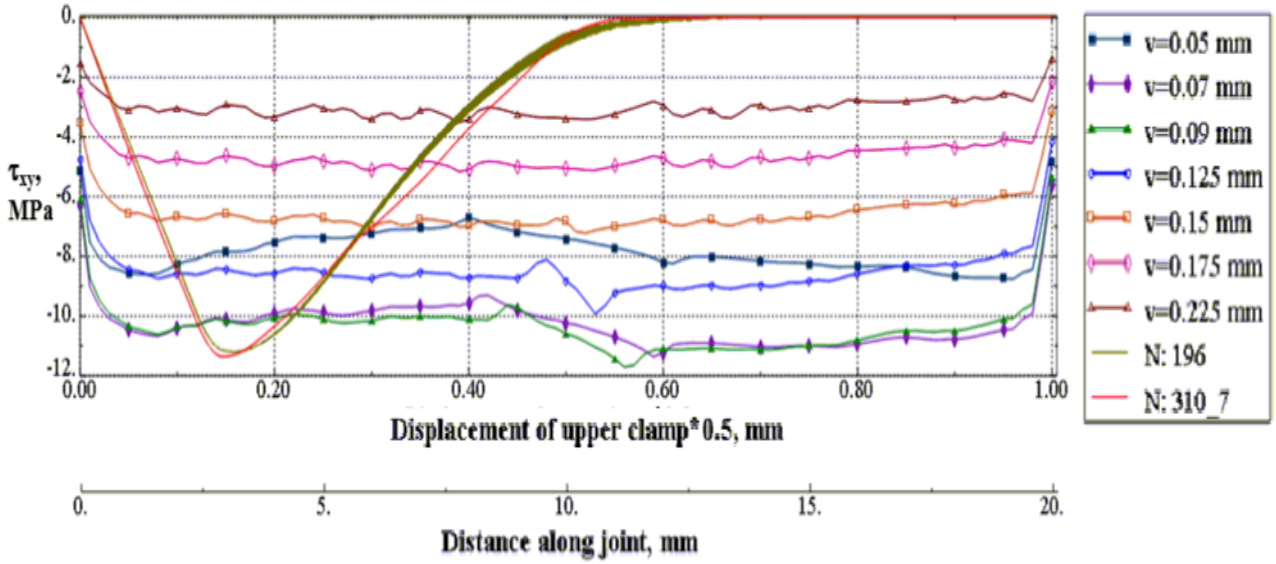

(a)

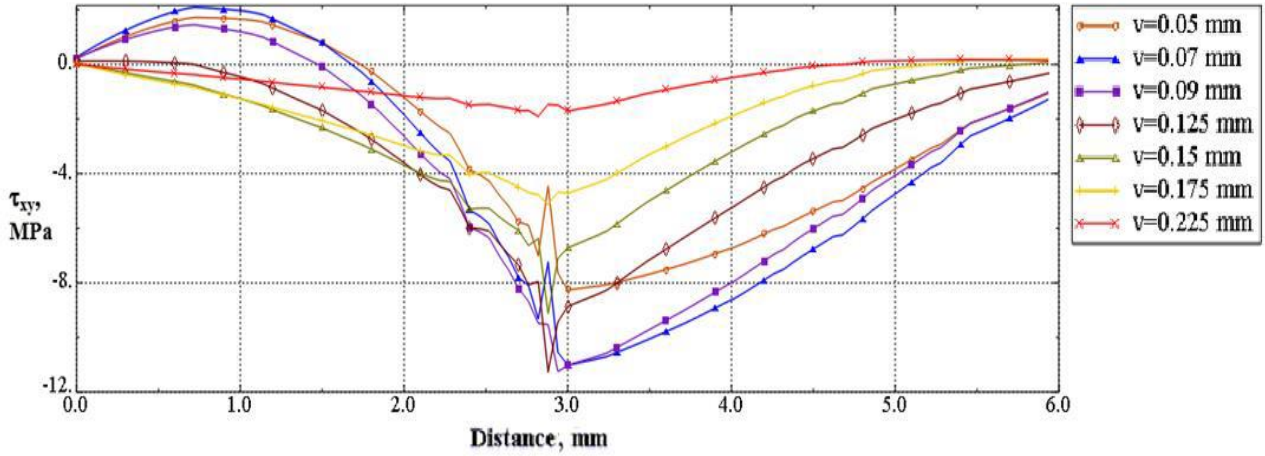

(b)

Fig. 36. Stress distributions along (a) in the adhesive joint and (b) perpendicular [4]

In the path along with adhesive bond figure in 36 (a), shear stress distribution looks enough even in all loading steps. Figure 36(b) shows the shear stress distribution in the bond area. The glue cohesive behavior is firmly related to elastic, strength and toughness of the joint [4].

4. DOUBLE LAP JOINT

4.1. Experimental techniques

By using of INSTRON E1000O electromechanical test machine the strength and durability of the carbon fiber bar rod glue joint were performed. Several different test specimens and load diagrams were prepared. The cross-section of the bars is square - 3.2x3.2 mm. Figure 37 shows the shape and dimensions of the samples. The length of the adhesive band of sample 37(a) was 40 mm. The specimens of this type were compressed in a special steel device, which was fastened to the test machine's receptacles. The working length of the unilateral and double-sided samples shown in Figures 37(b) and 37(c) was 20 mm. Figure 37(d) shows the sample used for fatigue testing. Longer chain type specimens were placed in square tubes containing polyethylene inserts. It was designed to give the stability of the sample during crushing. During the approval, the difference between the direction of the force and the axis of the test piece was not more than ± 0.5 °. For attaching the adhesive joint used epoxy resin and hardener. The samples after consolidation were maintained at a temperature of 80 ºC in a thermostatic environment for 3 hours or more. The static test load is 500 N / min and the cyclic load frequency is 20 Hz. Static and fatigue tests were performed in accordance with LST EN 2243-1 and LST EN ISO 9664 [1].

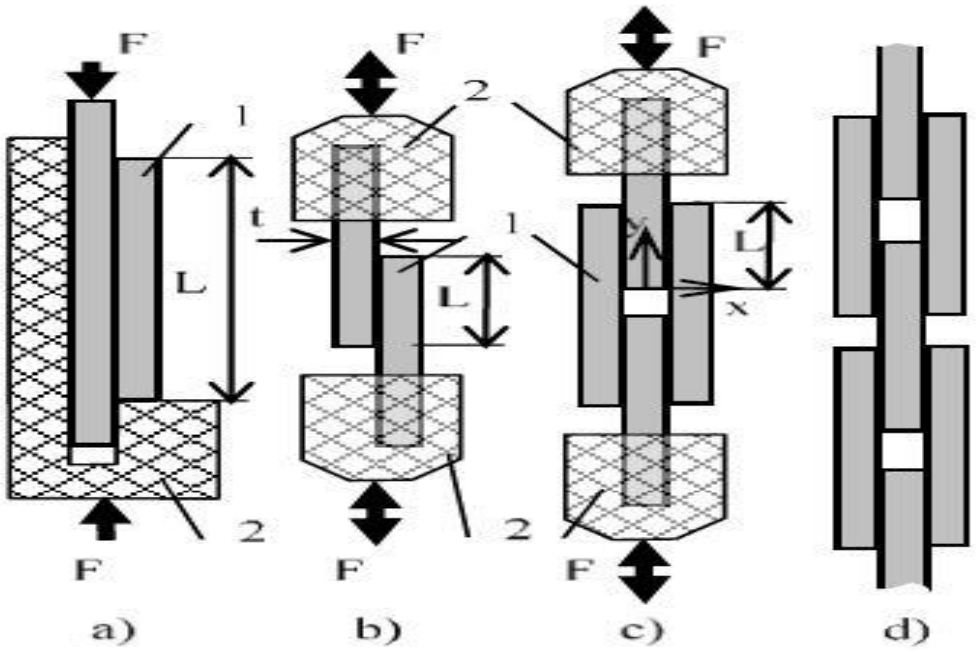

Fig. 37. View of specimens for static and fatigue tests [1]

4.2. Experimental results

The static test deformation diagrams are shown in Figure 38 is shown in Fig. 37 (a) specimen compression diagram, in which the strength of the samples at a temperature of 80 ºC for 7 hours is measured. Figure 38 (b) shows the tensile charts of other specimens. Also, Figure 38(a). A solid strain gauge is also provided [1].

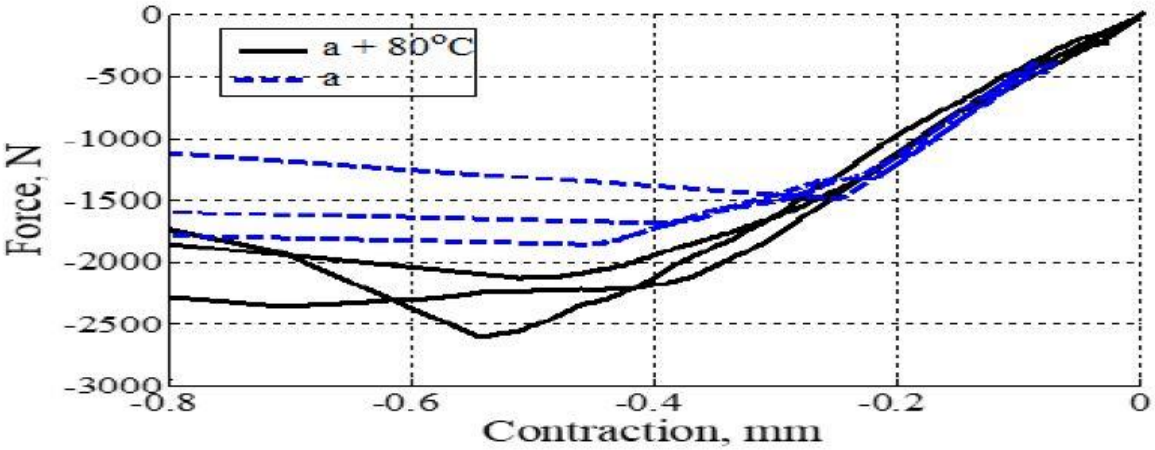

(a)

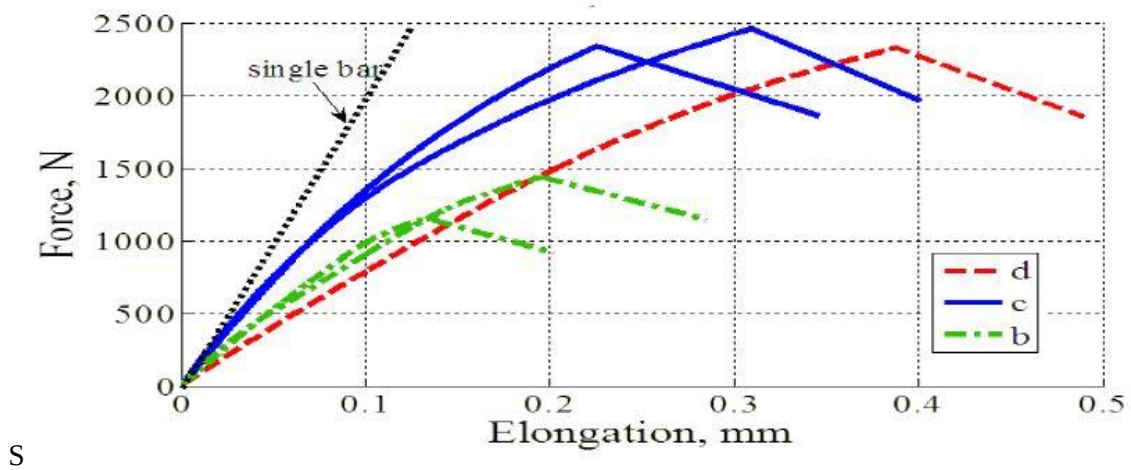

S

(b)

Fig. 38. Static test diagram of specimens [1]

The fatigue test was performed using single-sided and double-sided joints, as well as double-sided sample test chains (see Fig. 37). The fatigue test results are shown in Figure 39. The use of chain type (Fig. 37d) samples allowed the acceleration.

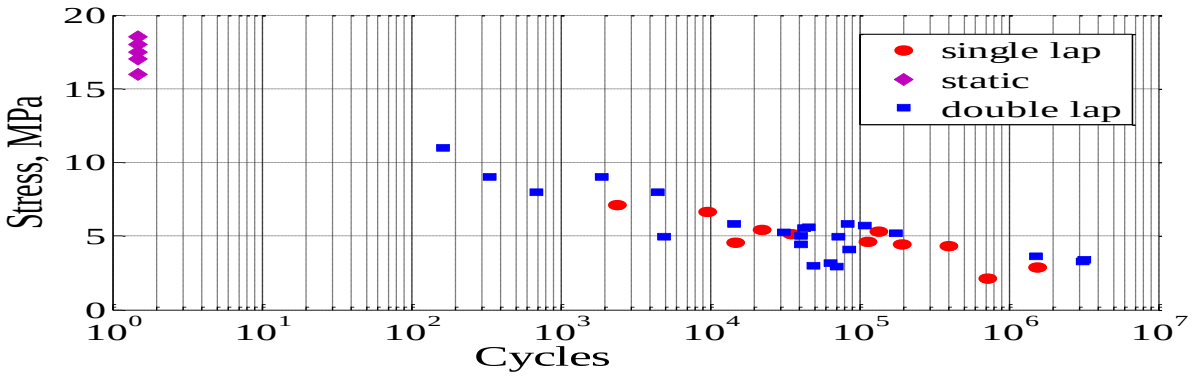

Fig. 39. Fatigue test results of a single lap, double lap and double laps chain specimens [1]

In fatigue tests, the load was kept at a frequency of 20 Hz with a cyclically varying force with a cyclic axial-metric coefficient of -0.5. The elongation of the specimen was measured according to the position of the upper tread of the test machine. During the test, load cycles were recorded in the following sequence: 1, 2, ... 10, 20, ... 100, 200, ..., 1000, 2000, ... The same sequence also captures the values of cyclic peaks and displacement values. One millennium of last cycles are saved when a test piece is lost.

According to the results of the fatigue test, the graph of the elongation dependence of cycles is calculated. Figure 40, A graph of one-sided adhesion connection is shown. It can be noted that decomposition occurs when the sample elongation increases by about 0.02 mm. The dependence of the connection deformations on the number of cycles can be described in terms of mathematical expressions and used to predict the decay motive of the joints [1]

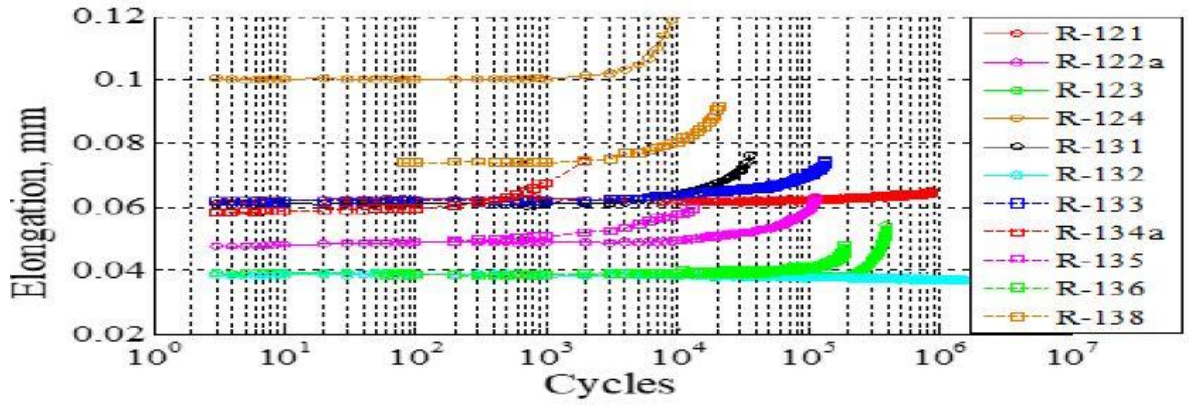

Fig. 40. Relationships of specimens' elongation [1]

The image of carbon fiber rod connections after static and fatigue fractures is shown in Figure 41. It can be noted here that the nature of the decay may be different. The irritation is adhesive, cohesive and mixed. On some occasions, decay occurs inside the carbon fiber rod.

Fig. 41. Views of adhesion zones after fatigue fracture [1]

The results of the test results show the peculiarities of the decaying of the carbon steel rods and the fatigue and it can be used to developing the strength of these glued joints. These tests were designed to test the available equipment and its ability to use carbon-fiber rod strength testing. Initial results

of tests for building and fatigue were obtained. Attention was drawn to the fact that the production conditions of the samples were important for the test results: surface preparation, the viscosity of the resin, hardening speed, compressive strength of the joints during the gluing, duration of the annealing of the joints and temperature. The variation of these parameters has a significant influence on the strength and durability of the building [1].

4.3. Analytical evaluation

The results of the test results show the peculiarities of the decaying of the carbon steel rods and the fatigue and can be used to develop the strength of these joints. These tests were designed to test the available equipment and its ability to use carbon-fiber rod strength testing. Initial results of tests for building and fatigue were obtained. Attention was drawn to the fact that the production conditions of the samples were important for the test results: surface preparation, the viscosity of the resin, hardening speed, compressive strength of the joints during the gluing, duration of the annealing of the joints and temperature. The variation of these parameters has a significant influence on the strength and durability of the building [1]. Calculated tangential tension of double lap joint by using formula number (5) which are 39.82, 31.25 MPa respected to 2500, 2000 N loads.

The average tangential tension in the contact area can be calculated as:

$$\tau_{xy} = \frac{F}{BL} \tag{5}$$

where F is a strength, B is the width of the bar, L is the length of the contact area. Distribution of tangential and normal stresses in the zone is uneven. The highest stress concentration is at the connecting staircase. Goland and Reissner proposed the following tangential and normal stresses of a one-way connection for elastic deformation of materials and conditions [1].

tG_a/t_aG <0.1 be tE_a/t_aE <0.1:

$$\begin{aligned} \tau_{xy}(y) &= -\frac{F}{4L}\left(\frac{\beta L}{2t}(1+3k)\frac{\cosh\left(\frac{\beta y}{t}\right)}{\cosh\left(\frac{\beta L}{2t}\right)} + 3(1-k)\right) \\ \sigma_x(y) &= \frac{4Ft}{\Delta L^2}\left(\left(R_2\lambda^2\frac{k}{2} + \lambda k'\cosh(\lambda)\cos(\lambda)\right)R_4(y) + \right. \\ &\quad \left. + \left(R_1\lambda^2\frac{k}{2} + \lambda k'\sinh(\lambda)\sin(\lambda)\right)R_3(y)\right), \end{aligned} \tag{6}$$

And

$$\beta = \sqrt{\frac{8G_a t}{Et_a}}, \qquad \lambda = \frac{L}{2t}\sqrt[4]{\frac{6E_a t}{Et_a}}, \qquad u_2 = \sqrt{\frac{3(1-\nu^2)}{2}}\frac{1}{t}\sqrt{\frac{F}{tE}}, \tag{7}$$

$$R_1 = \cosh(\lambda)\sin(\lambda) + \sinh(\lambda)\cos(\lambda)$$
$$R_2 = \sin(\lambda)\cos(\lambda) - \cosh(\lambda)\sin(\lambda)$$
$$R_3(y) = \sinh\left(\frac{2\lambda y}{L}\right)\sin\left(\frac{2\lambda y}{L}\right)$$
$$R_4(y) = \cosh\left(\frac{2\lambda y}{L}\right)\cos\left(\frac{2\lambda y}{L}\right)$$
$$\Delta = \frac{1}{2}(\sin(2\lambda) + \sinh(2\lambda))$$

where: t, t_a the thickness of the rod and the adhesive layer, E, G, Ea, Ga - the elastic and shear modulus of the connecting bars and the adhesive layer, v - the Puason coefficient of the rods.

During a periodic loading of the specimen, its deformation stays constant for a long period of time. They start to change when there is a crack in the contact area and an ever increasing gap. This is seen in Figure 37, the dependence of the length of the sample on the number of cycles can be expressed [1].

$$\delta(N) = a_1 e^{a_2 \lg N} + a_3 e^{a_4 \lg N} \quad (8)$$

Where N is the number of the cyc a_1,.....a_2 are the regression coefficients.

Table 4 is presented in Figure 30. The regression and correlation coefficients of the samples shown. We can see that, regardless of the number of decay cycles, the function given here describes the deformation dependence on the number of cycles. Assuming that the resulting limiting deformation δω is the same for all loading levels that correspond to the initial deformation δ_0, we can calculate the number of decay cycles N_u well from the equation.

$$\delta_u - \delta_0 = a_1(e^{a_2 \lg N_u} - e^{a_2}) + a_3(e^{a_4 \lg N_u} - e^{a_4}) \quad (9)$$

Table 4. Fitting parameters of single lap adhesion bound of carbon fiber bars [1]

Spec	Nu	Fitting coefficients and their confidence bounds				R2
		a_1	a_2	a_3	a_4	
R141	700	0,118 (0,115; 0,1208)	-0,0490 (-0,0678; -0,0301)	2,39e-05 (2,54e-06; 4,54e-05)	2,49 (2,21; 2,78)	0,999
R138	21000	0,0742 (0,0732; 0,0752)	-0,00181 (-0,00785 ; -0,00422)	9,72e-08 (-3,78e-08; 2,32e-07)	2,79 (2,47; 3,10)	0,995
R143	1156000	0,0334 (0,0332; 0,0337)	-0,00598 (-0,00770; -0,00426)	2,91e-12 (1,81e-12; 4,01e-12)	3,65 (3,59; 3,71)	0,992

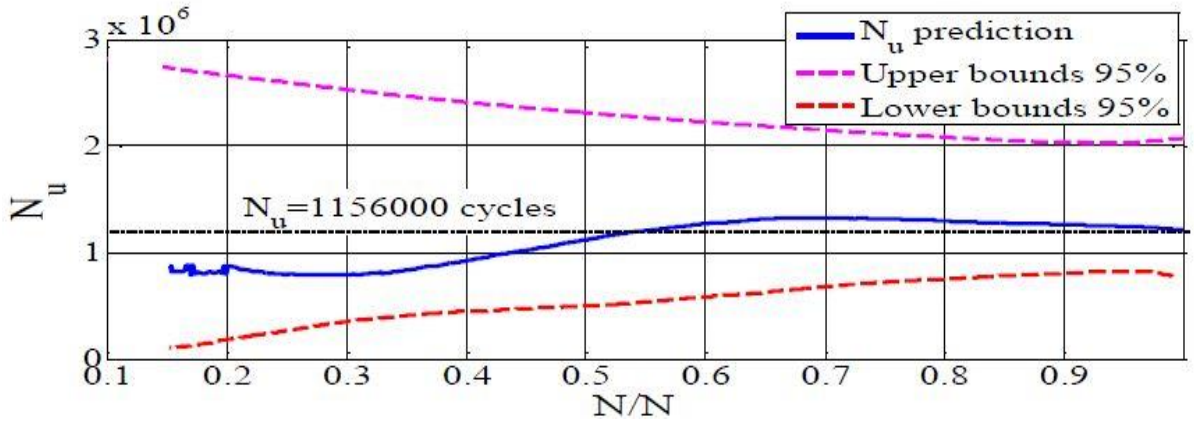

Fig. 42. Prediction accuracy of an adhesive bounds lifetime [1]

Figure 42 shows how the expected longevity of the connector in the course of the test varies according to the results of the sample deformation measurements. Here are also the 95% confidence limits predicted by the MATLAB program. From them, it is seen that precise predictions of fracture momentum are obtained from half the number of cycles corresponding to the fracture of the sample. This indicates that deformation measurements can provide a resource for such connections. The presented dependencies, which predict the adhesion stresses. In these dependencies, the mechanical properties of the materials, the geometry of the joint and the nature of the load are evaluated [1].

4.4. Numerical studies

Analytical models are important in order to understand and describe the state of adhesive joints, the distribution of stresses and deformations, the influence of geometric parameters and material properties on the strength and durability of adhesive joints. They are also useful today for rapid analysis of both research and industry needs. However, a more precise evaluation of connectors is possible when numerical methods are used [1].

In this work, the ABAQUS program was used for calculations and a cohesive zone model was introduced in it. This way is convenient, relatively compact in terms of memory and time resources. The boundary state of the cohesive zone is defined by this condition:

$$f = \tau - \sigma_0 tg\beta - d = 0, \tag{10}$$

Where f is the state function, t tangent stress, $\sigma_0 = \frac{\sigma_1+\sigma_2+\sigma_3}{3}$ is the hydrostatic stress, d is the cohesive parameter, β is the friction angle, $\sigma_1, \sigma_2, \sigma_3$ - the principal stresses. Graphically, this can be illustrated in Figure 13. shown schema The expansion angle φ and the change in non-elastic deformation $d\varepsilon^{pl}$ are related:

$$d\varepsilon^{pl} = d\bar{\varepsilon}^{pl} \frac{\tau_\alpha}{\tau} \cos\psi \, \mathbf{n}\cdot\mathbf{n} + d\bar{\varepsilon}^{pl} \sin\psi \, (\mathbf{n}\cdot\mathbf{t}_\alpha + \mathbf{t}_\alpha \cdot \mathbf{n}) \tag{11}$$

here $d\bar{\varepsilon}^{pl}$ is the value of the change in non-elastic deformation, and n and tα are normal and tangent to the tangential direction of the cohesive surface ∝. The cuff link is assumed to be uniform and

immobile when f<0. The decomposition of the connection occurs when the state function becomes zero to f=0.

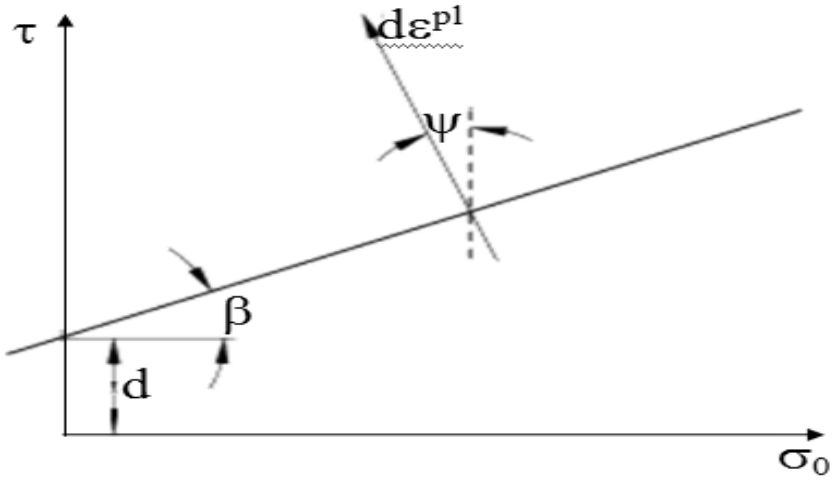

Fig. 43. Constitutive state of cohesion zone [1]

In the ABAQUS FEA system, coherent interaction is defined as a surface interaction property and can be applied to simulate layering. The decay of interactions is described by the state of its initialization and its degradation properties. The mechanical properties of the interaction are characterized by its stiffness and strength, as well as by the behavior of the beginning of the decay. The mechanical properties of the collaboration are portrayed by its solidness and quality, just as by the conduct of the start of the rot, Which is depicted by the vitality and uprooting parameters.

Figure 43, The possible dependencies of the interaction stresses (t), displacements (δ) and energy (G) are schematically shown [1].

In this work, the connection was modeled in 2D space using flat squares and triangular finite elements. Analysis of the two-sided and one-sided samples of the adhesive joint, shown in Fig. 44

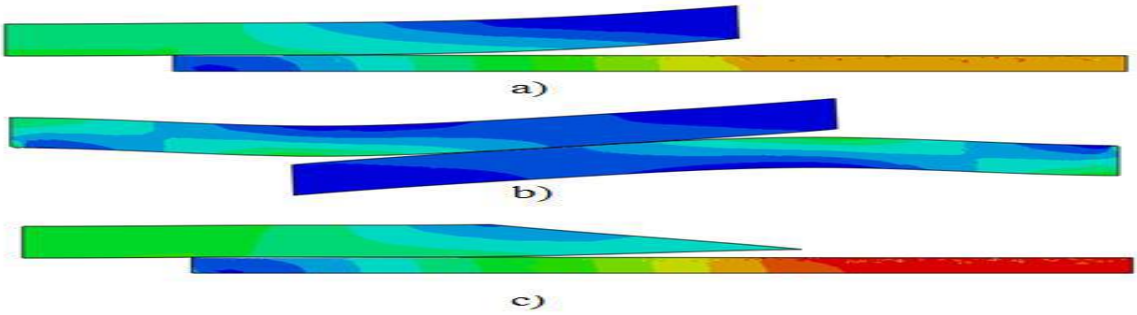

Fig. 44. Deformation of the double lap (a), single lap (b) and inclined double lap (c) joints [1]

The double-sided joint sample was taken with respect to the symmetry longitudinal axis. Contact Interface - "Cohesion behavior" and "Damage". The carbon steel rods are deformed differently in single-sided and double-sided joints. In the unilateral connection due to a significant bending moment, significant normal stresses perpendicular to the axis of the beam appear. The great influence on the state of stresses and the nature of the degradation is due to the initialization of the decay and the continuation of the course of the work - this is thoroughly examined. Figure 45 shows

the shear stress distribution in the contact area with a two-way connection and elastic deformation is demonstrated. The level of stress concentration strongly depends on the stiffness of the adhesive connection. In the case of rigid couplings, the high tensile imbalance is obtained, and when the stiffness corresponds to the properties of the epoxy resin, the stress distribution is quite even. The calculations were made by changing the stiffness of the adhesive joint K [1].

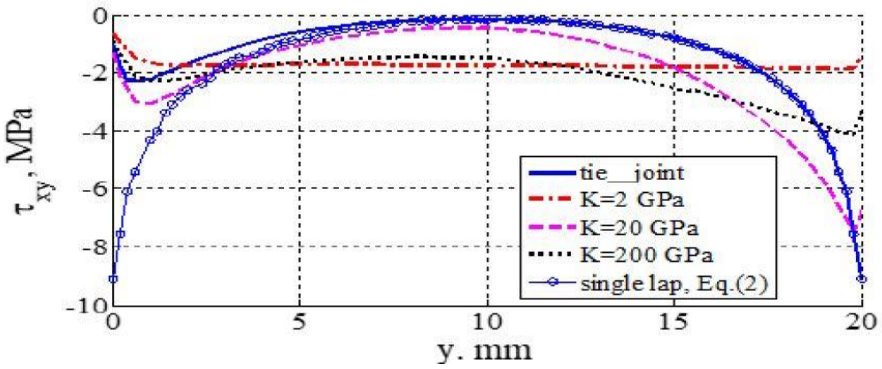

Fig. 45. Shear stress distribution along contact zone [1]

The calculations of static and fatigue were also performed, and the decay of the adhesive joint was analyzed. Fig. 46 (a) is shown how the deflection loops in two-sided connections change in the course of decomposition when the slit increases and the connection is decomposed in 20 cycles. Fig. 46 (b) An INSTRON E10000 test machine for a test piece that has broken down after 10,000 cycles are provided for a two-way coupling test. The numerical model displacement begins to increase rapidly after reaching the 0.015mm displacement. In the real case, the connection will break after this displacement.

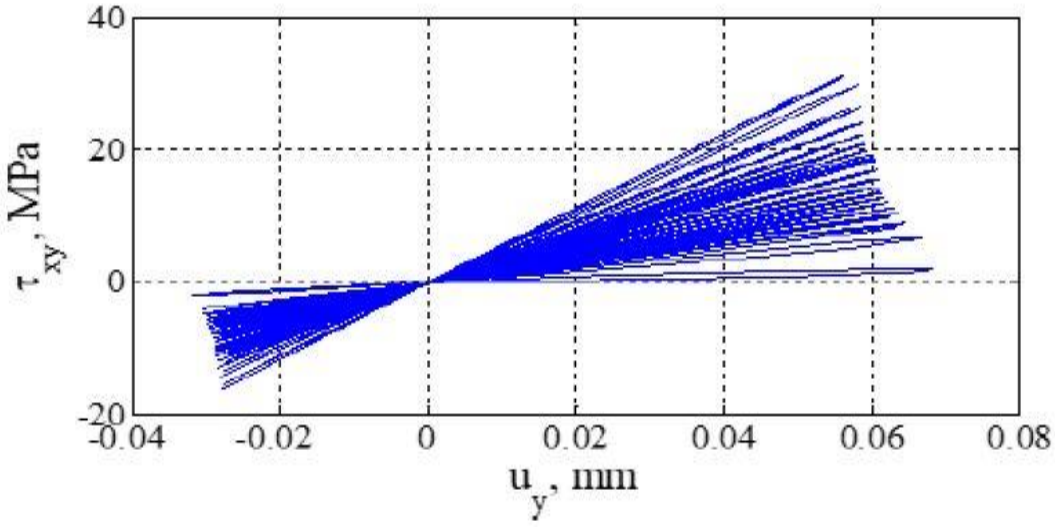

(a)

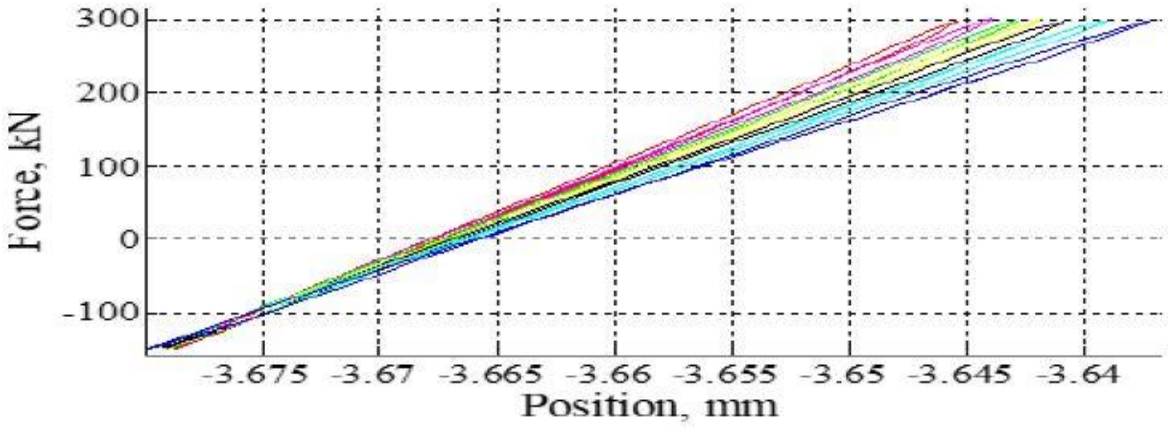

(b)

Fig. 46. Shear stress distribution on the contact area [1]

The examination comes about an exhibit that glue peel stresses are the greatest among all the pressure parts, and the shear and peel worries of the adhesive are the most imperative segments. Because of the pressure peculiarity, peak stresses happen at the joint corners. The disfigurement and prolongation happen when the load increments keeping in mind the end goal to watch the peel pressure and shear pressure are depended upon the glue thickness and material properties. Reviewed ultimate forces and stress along with the specimen and it‘s deformation when changed the adhesive thickness and material properties. Observed various results and deformations. Reduce the deformation percentage by using proper glue viscosity and overlap length of the joint [1].

5. Three-Dimensional joints

5.1. Adhesive Material and applications

There are two clams and adhesive is required for joining. The material selected for adherence is carbon fiber and adhesive is an epoxy resin. For increasing joint efficiency, the rheological properties of adhesive material should be quite similar to that of adherends. Different types of glues are using in the manufacturing industries, which are Epoxy, polyester, resins, nitric rubber, phenolics. In this epoxy is frequently used for mechanical purpose because of their high internal strength in cohesion, low shrinkage stress, requires the low temperature to cure and creep, intensity to moisture, no crevice corrosion, good damping properties. The main reason uses this type of joints because it's fast and cheap joining, and having nature of uniform stress distribution, its capable of joining large structures and different materials. In the aircraft, adhesives are used for spar connections, wing structures, bonding strangers and the structure of honeycomb cores inside for the control equipment structures such as elevator, ailerons, spoilers [19].

5.2. Configuration of adhesively bonded joints

The shear lap and double lap joints which are bonded with the help of the adhesive is shown in figure 47. Two same type adherents are used for one-side and two-sided joints, which is carbon fiber rods. The following values were used for this; overlap = 20mm, rod thickness = 3mm, Adhesive thickness is 0.02 mm. Nonlinear behavior of the geometry and material properties were considered for one-side and two-side joints. The overlap length of the double lap balanced and unbalanced is 15mm, performed in Abaqus software with 2500 N force.

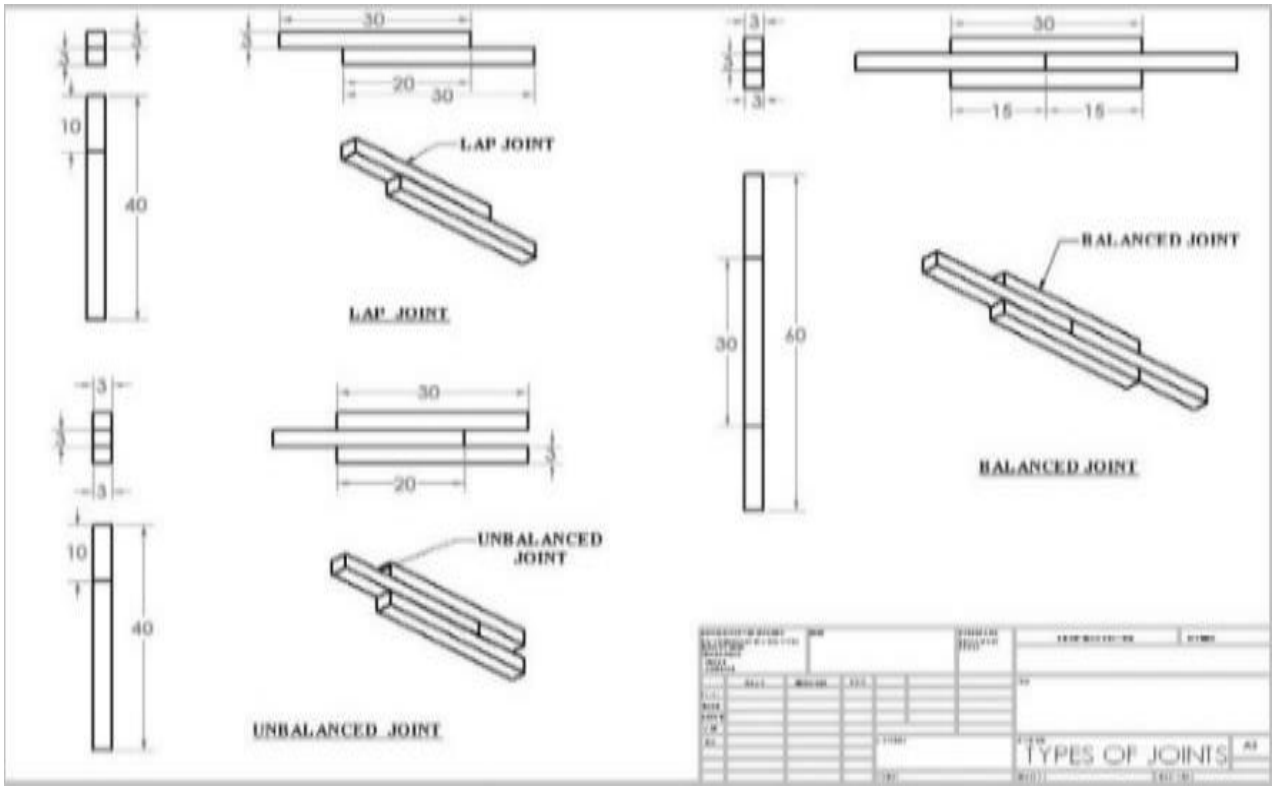

Fig. 47. Drawing of different adhesive bonded joints

5.3. Methodology

The shear lap and double lap balanced and unbalanced joints were analyzed in ABAQUS student version. In that design and analysis have various methods for the analysis of lap joints which are solid, shell, beam, Gasket, and cohesive sections. Different types of analysis chosen a solid section to obtained results of a single bar and double lap balanced and unbalanced joints. Based upon analysis chosen best mesh in terms of accurate results in Abaqus student version for these type of connections are Hex-structured. Mainly two different type of constraints are famous which are surface to surface interaction and Tie contain. This tie contact bond connects the surfaces as one pair during the simulation which can be subjected to mechanical loads, coupled temperature-displacement, coupled thermal-electrical-structures. In the case of self contact and defining contact properties, it cannot be used. Surface to surface standard interaction is the best for obtaining adhesive strength of the single side and two-sided joints [28].

5.4. Numerical Simulations

The least difficult investigation considers the adherends to be rigid and the adhesive to deform only in shear this appears in figure 48. Calculated shear stress of the shear lap along the adhesive joint the maximum forces is 1500 N and stress acting on the adhesive joint is 25 MPa and the double lap is about 2500N and shear stress acting along the joint is 41.6 MPa.

The shear stress τ of the lap joint is given by

$$\tau = \frac{P}{bl} \tag{12}$$

For adherend tensile failure outside the joint

$$P = \sigma_y t \tag{13}$$

For adhesive shear stress failure.

$$P = \sqrt{8E\tau_P\eta(\frac{\gamma_e}{2} + \gamma_P)t\alpha\sqrt{t}} \tag{14}$$

where σ_y is yield stress of adherend, t is the thickness of adherend, E Young's modulus of the adherend, τ_P is plastic glue shear stress, P is loading, the η is the adhesive layer thickness, γ_e is Elastic adhesive shear strain, γ_p Plastic adhesive shear strain. E_c' adhesive peel modulus, b is the width of the joint, L is the length of the joint [(1)].

Inter-laminar normal and shear stress(σ_y) once used in the failure criterion for tensile and compressive peel stress condition;

$$\sigma_\gamma > 0$$

$$(\frac{\sigma_\gamma}{R_T})^2 + (\frac{\tau_{\gamma z}}{S_{\gamma z}}) + (\frac{\tau_{\gamma\theta}}{S_{\gamma\theta}})^2 = e_d^2 \quad \begin{cases} e_d^2 \geq 1, \ failure \\ e_d^2 < 1, no failure \end{cases} \tag{15}$$

$$(\frac{\sigma_\gamma}{R_C})^2 + (\frac{\tau_{\gamma z}}{S_{\gamma z}}) + (\frac{\tau_{\gamma\theta}}{S_{\gamma\theta}})^2 = e_d^2 \quad \begin{matrix} \{e_d^2 \geq 1, \ failure \\ e_d^2 < 1, no failure \end{matrix} \tag{16}$$

Where σ_y, τ_{yz}, τ_{yx} are interlaminar Peel and Shear stress components. R_T, R_C, S_{yz} and S_{yx} are the strength components in the corresponding direction. e_d is the adhesive failure or delamination damage index is used to locate the adhesive failure in spar [(2)].

5.5. Finite element simulation:

The mesh size also various in results and type of mesh influence the results, for this type of connections Hex-structured is the best for getting proper results and mesh size 1 because Abaqus student version allowed me up to 1000 nodes not more than that. The software Abaqus was considered evaluating the stress and delamination of the shear lap and double lap balanced, unbalanced joints and suggesting the best connections for sailplane spar design. The meshes for all FE models were automatically created by the software.

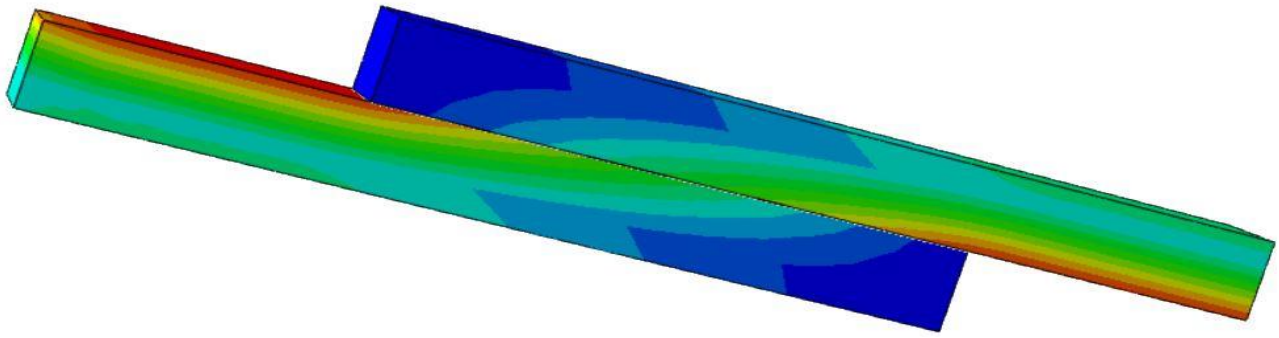

Fig. 48. Three-dimensional single lap joint

Above figure red colour shows that connection is not in shear but under peeling stress at the end of the connection. Moreover, adherends are not under tensile stress but are bent. Adhesive and adherend have plasticity at high-stress concentrated areas. Although, the used high strength carbon fiber rods as adherents for One-side and two-sided joints, shows that plastic deformation due to rotation causes the Failure.

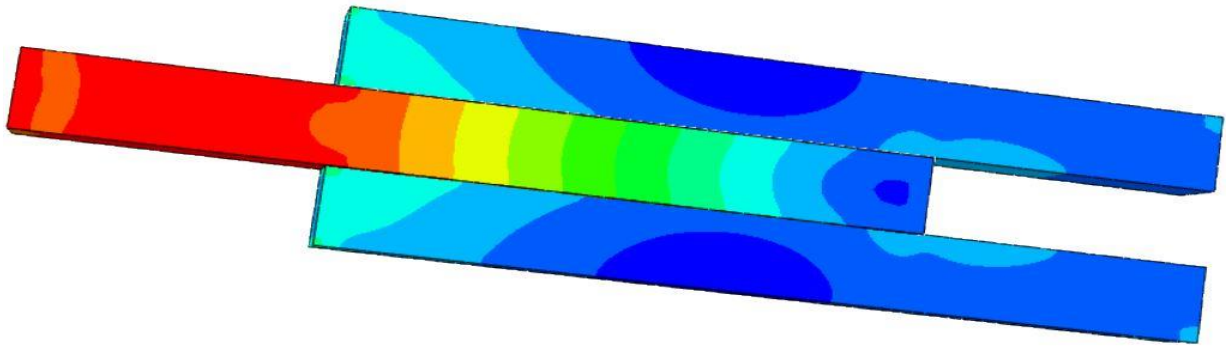

Fig. 49. Three-dimensional unbalanced double lap joint

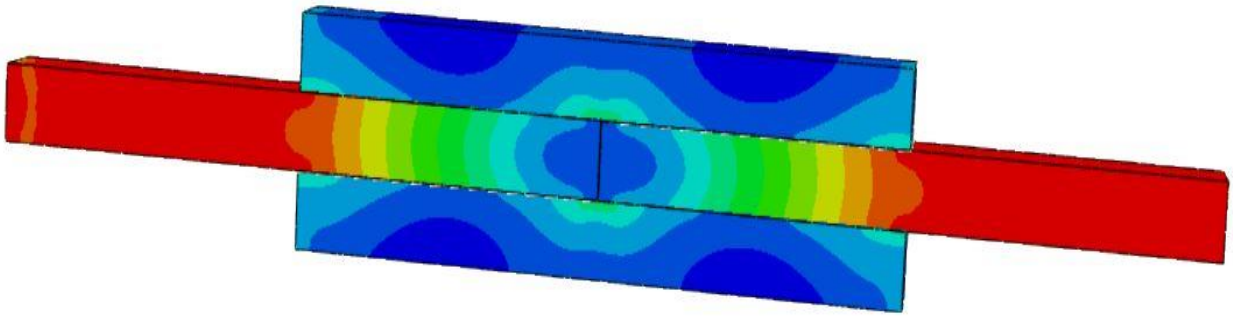

Fig. 50. Three-dimensional balanced double lap joint

In the above figure, double lap joints are used to be said that bending effect could be eliminated and as no more rotation of connection. This joint designed to improve load transfer and reduced stress concertation and peel. The double lap joints made with same adherents, adherents tensile failure outside the joint. FE investigation shows the concentration of stress is in the glue layered of a lap joint not only but nearby to the closures to the bond. But in the locale of the edge of the less load concentrated adherend. The proposal, might conceivable for the joint yield strength to raise the edge of the adherend. The Adams and peppiatt in the year 1974 have analyzed for 0.4 mm on the emptied adhere corner and the maximum principal stress in the spew was much lower then acquire with Perpendicular corner [25]. Interlaminar stresses happen at the joint interfaces because of the impact of coupling and furthermore longitudinal displacement increments. As shown in the double lap joints predicted higher stress and also crack propagation. For sailplane spar connection both balanced and unbalanced joints will be good.

Figure 51(a) shows that stress distribution over upper adherend and the lower adherend. Observed that near adhesive bond area high stress (at displacement 0.07mm)are presented along the adherend and stresses keep on decreasing from adhesive layer area. The same situation was in the double lap joints.

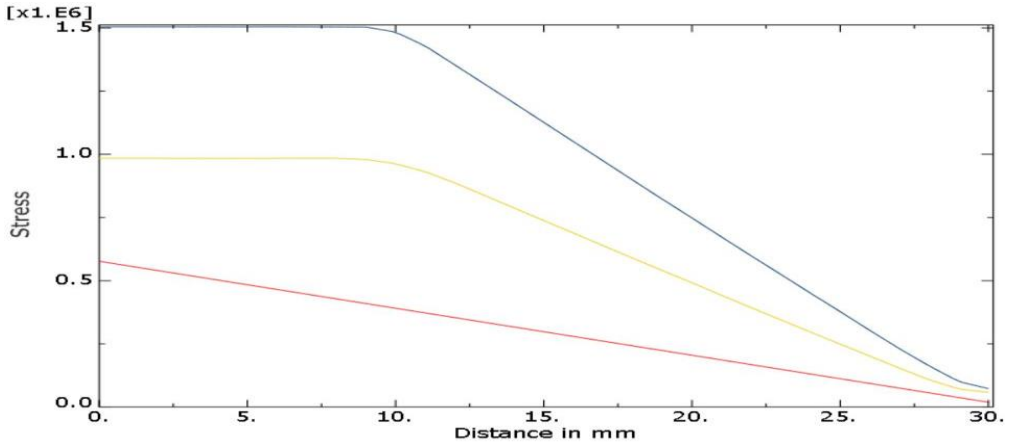

Fig. 51. Stress distribution over a single lap

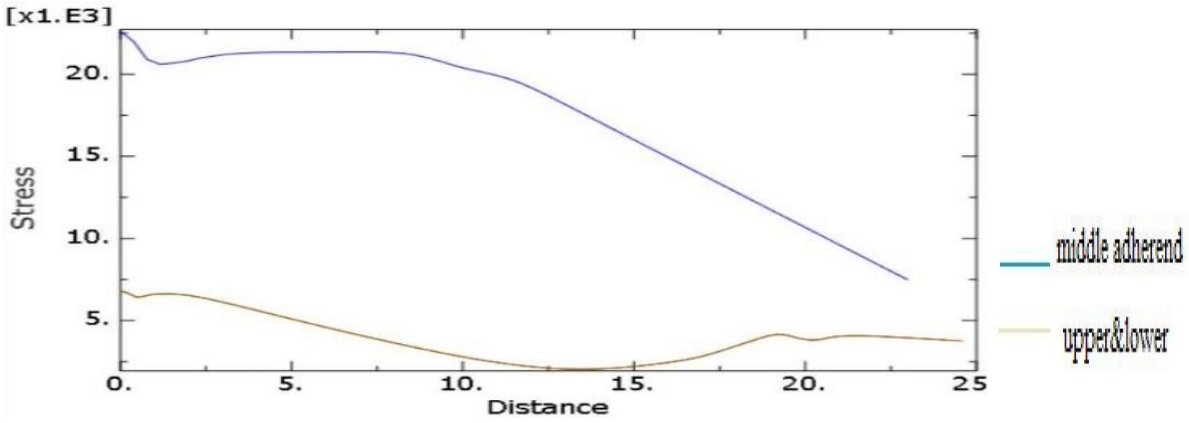

Fig. 52. Unbalanced double lap joint stress distribution

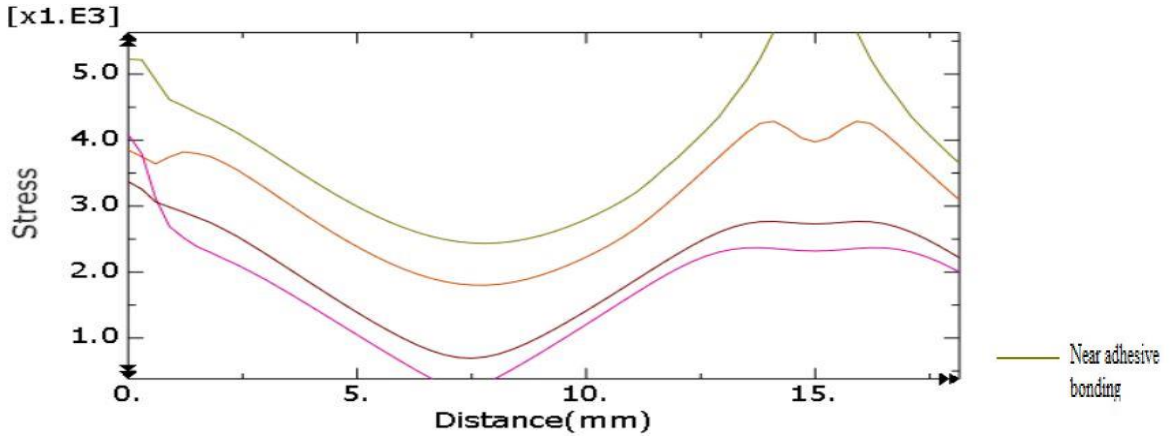

Fig. 53. Balanced double lap joint stress distribution

5.6. Wing static analysis

The double lap balanced and unbalanced joints wing connections were analyzed in Solid works student version. In that design and analysis have performed with a 15m length of the wing, in that 615mm is the spar length, chord length is about 612mm, the applied load is 1000 N in both cases. Based upon case studies chosen the best software for basic understanding about the structures and it‘s moments.

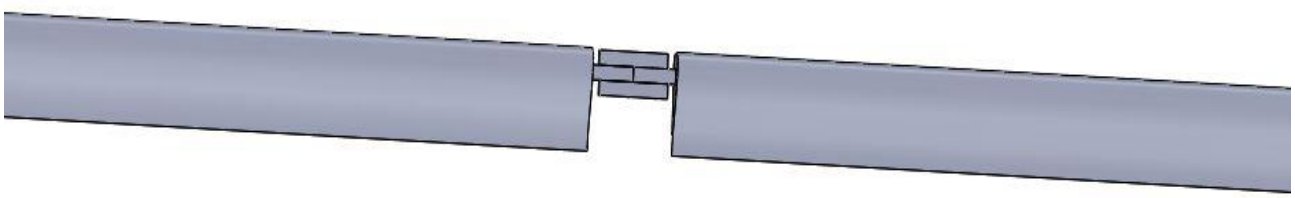

Fig. 54. Sailplane model wing with double lap balanced joint

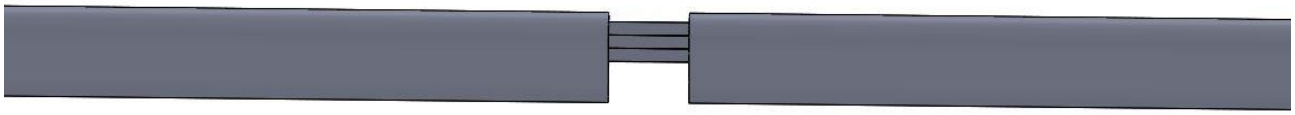

Fig. 55. Sailplane double lap unbalanced wing

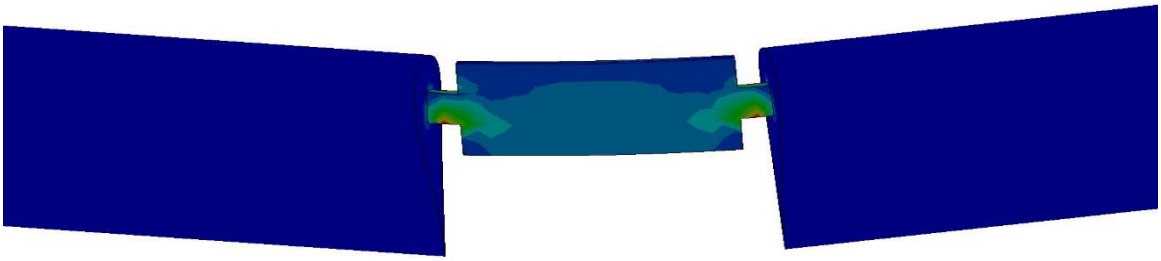

Fig. 56. Double lap balanced joint wing static analysis

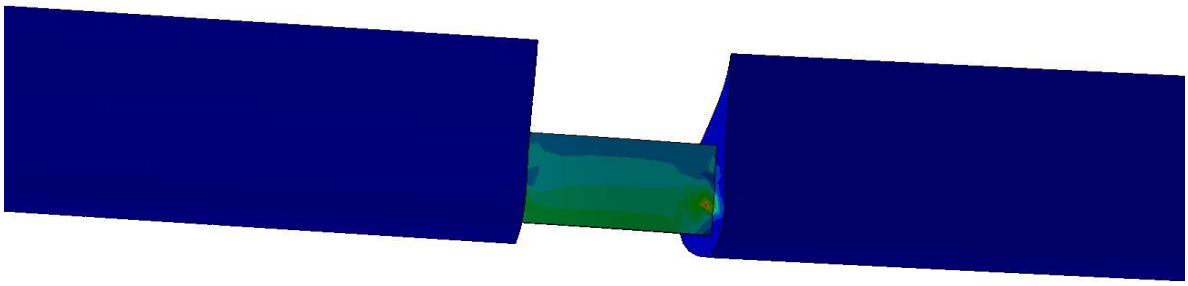

Fig. 57. Double lap unbalanced joint wing static analysis

The Analysis of the wing with Unbalanced(figure 57) and Balanced(figure 56) joint is being tested using Solidworks software with appropriate values to evaluate the stress concentration at the spar connection joints. The analysis is carried by fixing the outer edges of the wing as to test the strength of the joint by loading on to bar faces. The results show that the unbalance joint is less vunrable compared to balance joint. From observations, the stress concentration is at the edges of unbalanced joint whereas for the balanced joint the stress concentration is at the closer side of the wing of the main bar but not on the overlapped bars. The stress developed is at the connection but not throughout the bar. However, the concentration of the stress in the unbalanced joint is more in the connected region whereas in the balanced joint the concentration of stress is limited at both end regions of the joint but not in entire joint connection.

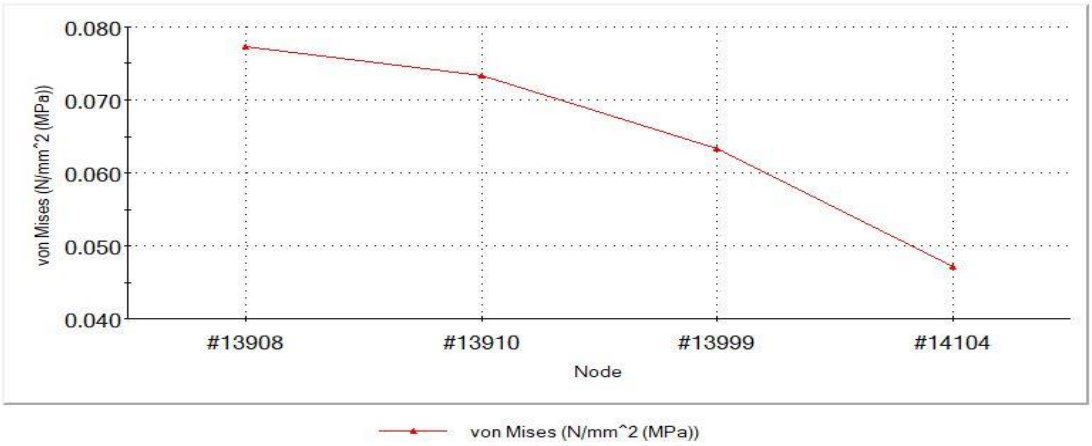

Fig. 58. Stress distribution in the balanced joint wing

Figure 58 elaborates the stress distribution in the balanced joint, Observed that stress is gradually going downwards as we move beyond the edges i.e., from ends to the center of the joint.

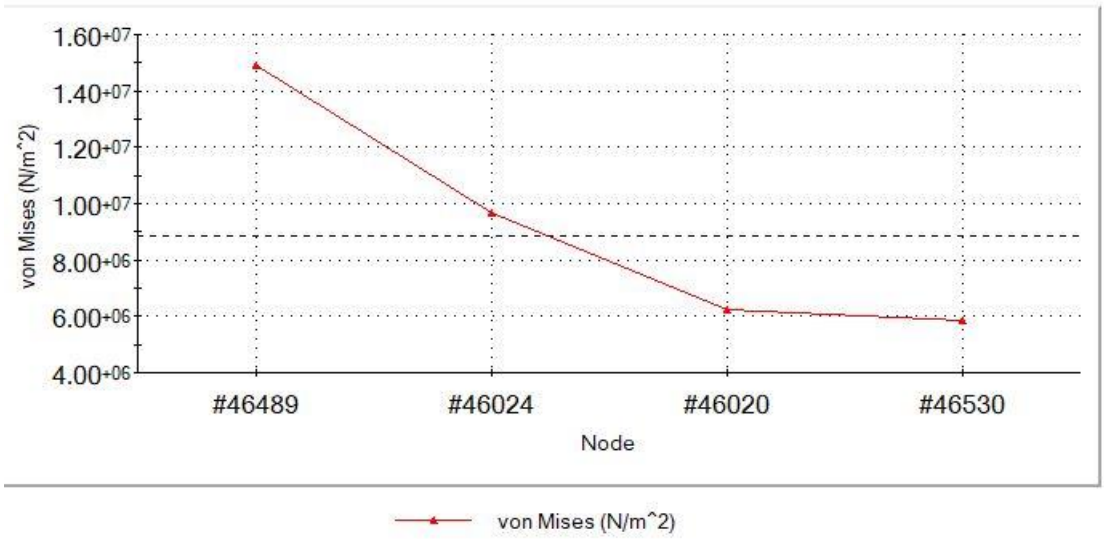

Fig. 59. Stress distribution in the balanced joint wing

The above graph represents the unbalanced joint, the stress distribution drops as the move from edges to the middle of the joint but as compared to the balanced joint the stress is reduced at a lower rate to unbalanced joint and further observed that stress is linear at the center and goes up while reaching to the end of the joint.

Conclusion

In this research work, the ultimate strength, stiffness, deformation or cracking of adhesive bonding in carbon fiber shear lap joint was analyzed. Found the best overlap length is about 20 mm and maximum force can withstand the joint is 1437.33 N (static analysis) in a single lap joint and the maximum displacement of the upper clamp is 0.5 mm.

As of the end of the structural analysis, the complete deformation of the double-lap joint will be found after 10,000 load cycles and decomposition in 20 cycles.

By numerical evaluation observed the displacement of 0.015 mm after this started increasing rapidly. The strength and durability of the joints were monitored and experimental and quasi-analytic strength of single-sided and double-sided connections and Some peculiarities of the connections like the breaking of one side of the joint at the 22.45MPa, affect the bending strength.

Deformation diagrams and fatigue curves of the tested specimens are presented. The long chain double lap specimens for fatigue test is proposed, what provides opportunities for accelerated fatigue experiments and also allows obtain a more reliable statistical assessment.

The well-fitting function of experimental results for prediction of lifetime of joints is developed. Presented simulation of the sailplane spar connections single lap, double lap balanced, and unbalanced joint were performed in Abaqus software.

Analyzed the structural influence in adhesive and adherend at various regions. During the simulations of these connections observed the higher stress near the adhesive layer and damage occurs inside the adherend, found the delamination s in the joints.

The crack propagation in the joints will be increased by increasing the load. By using these results, Suggested the best connection of the spar is balanced double lap joints. This joint will help in terms of stress reduction in adhesive bonding connections and delamination.

The prepared ABAQUS and MATLAB models well describe the strength and durability of the joints and also these results shows the bonding strength of the adhesive joints can be used for design and technical diagnostics.

Researches, experiments, and their results were presented in articles at scientific conferences. Analysis of adhesive bonding in carbon fiber bar single lap joint at the ‘‘Young scientists conference‘‘ 2018. Strength and Durability of Carbon Fiber Bar Adhesive Bonding at the ’’Mechanics 2018 conference’‘. Finite element approaches to simulate the different types of sailplane spar connection at the International ’‘Young Scientists Conference 2019‘‘ (see Appendix).

References

1. **Rokas GUDELIAUSKAS, Martynas LENDRAITIS, Naga Manikanta KOMMANABOINA, Kazimieras PETKEVIČIUS,** Strength and Durability of Carbon Fiber Bars Adhesive Bonding. Mechanika 2018. Kaunas: Kaunas University of technology, 2018.
2. **Daniel Marcus GLEICH**, Stress analysis of Structural bonded joints, Imperial College in London.
3. **Johan Ekh**, Multi-Fastener Single-lap Joints in Composite Structures, Department of Aeronautical and Vehicle Engineering, Royal Institute of Technology, SE–100 44 Stockholm, Sweden,
4. **Naga Manikanta Kommanaboina, Hari Prasanna Manimaran, Mastan Raja Papanaboina, Kazimieras Petkevičius**, Analysis of carbon fiber bar in single lap joints. young scientists conference 2018: Kaunas University of technology, 2018.
5. **Fabrice Lapique*, Keith Redford**, Curing effects on viscosity and mechanical properties of a commercial epoxy resin adhesive, International Journal of Adhesion & Adhesives 22 (2002) 337–346.
6. **Mr. Khapare S. A.1, Prof. Gaikwad M. U**., Validation of Double Lap Adhesive Joint for Al-Al Plates.
7. **Anirudh Narayan**, **Giulio Alfano,** Conceptual Design of a Carbon-fibre Composite Aircraft And Finite Element Analysis of the Wing, Advanced Mechanical Engineering Brunel University, West London.
8. **Paul W. Harper, Stephen R. Hallett**, Cohesive zone length in numerical simulations of composite delamination.
9. **Prof. R. Aravind, Dr. M. Saravanan, R. Mohamed Rijuvan**, Structural Analysis of Spar Made-up of Carbon Fiber Composite Material (International Conference on Interdisciplinary Engineering & Sustainable Management Sciences (ICMIE'13) on 22nd & 23rd February 2013).
10. **J. Kupski, S. Teixeira de Freitas, D. Zarouchas, P.P. Camanho, R. Benedictus**, Composite layup effect on the failure mechanism of single lap bonded joints.
11. **D.M. Gleich, M.J.L. van Tooren and A. Beakers (2001),** Analysis and evaluation of bondline thickness effect on failure load in adhesively bonded structures, Accepted for publication in J. Adhesion science and Techno. 15(9), 1091-1101.
12. **P.J. Gray, C.T. McCarthy**, A global bolted joint model for finite element analysis of load distributions in multi-bolt composite joints,
13. **Elena M. Moya-Sanz, Inés Ivañez, Shirley K. Garcia-Castillo**, Effect of the geometry in the strength of single-lap adhesive joints of composite laminates under uniaxial tensile load, International Journal of Adhesion & Adhesives 72 (2017) 23–29.
14. **Stefano Carrino, Francesco Nicassio, Gennaro Scarselli, Raffaele Vitolo**, Finite difference model of wave motion for structural health monitoring of single lap joints, International Journal of Solids and Structures 161 (2019) 219–227.
15. **Sun Zhenqi, Huang Minghui, Lu Xinjiang**, A Cohesive Zone Model in Adhesive Bonding Joint Based on MSC.marc.
16. **Campilho, R**.2017. Strength Prediction of Adhesively Bonded Joints. CRS Press Tylor & Francis, 422P.

17. **A.M.G. Pinto, R.D.S.G. Campilho, I.R. Mendes and A.P.M Baptista**, Numerical and experimental analysis of balanced and unbalanced adhesive single lap joints between Aluminum adherents.
18. **P. K. Mishra, A. K. Pradhan & M. K. Pandit**, Delamination propagation analyses of spar wing skin joints made with curved laminated FRP composite panels.
19. **Harshada M. Ahire, Sumit R. Singh**, Adhesive bonding of aircraft structures (International Journal for Research in Applied Science & Engineering Technology [online] IJRASET [accessed march. 2018]. Available at www.ijraset.com.
20. **Mr. Khapare S. A., Prof. Gaikwad** M. U, Validation of double lap adhesive joints for Al-Al plates.
21. **L.J Hart- smit**, Adhesive bonded double lap joints.
22. **Nikola Petrasinovic, Bosko Rasuo, Danilo Petrasinovic**, Aircraft Dialuminium wing spar.
23. **Wilson A. Perez,** Finite element method simulation of single lap shear tests utilizing the cohesive zone approach.
24. **Xiaocong He**, Effect of mechanical properties of adhesive on stress distribution in structural bonded joints.
25. **Robert D. Adams, William C**. Wake, Structural adhesive joints in Engineering.
26. **M.Y. Tsai, J. Morton,** An investigation into the stresses in double-lap adhesive joints with laminated composite adherends.
27. **Marek Orkisz, Łukasz Święch, Jan Zacharzewski**, Fatigue tests of motor glider wing's composite spar.
28. ABAQUS Documentation. [accessed 9 Febr. 2018]. Available from Internet: http://abaqus.software.polimi.it/v6.14/index.html.
29. **Jinxin Ye, Ying Yan, Jie Li, Yang Hong, Ziyang Tian,** 3D explicit finite element analysis of tensile failure behavior in adhesive-bonded composite single-lap joints. Composite Structures 201 (2018) 261–275.
30. **Iordanis T.Masmanidis, Theodore P.Philippidis,** Progressive damage modeling of adhesively bonded lap joints. InternationalJournalofAdhesion&Adhesives59(2015)53–61.
31. **Siddharth Pitta, Victor de la Mora Carles, Francesc Roure, Daniel Crespo, Jose I. Rojas,** On the static strength of aluminum and carbon fiber aircraft lap joint repairs. Composite Structures 201 (2018) 276–290.
32. **Florin Adrian Stuparu a, Dragos Alexandru Apostol,** Local evaluation of adhesive failure in similar and dissimilar single-lap joints. Engineering Fracture Mechanics 183 (2017) 39–52.
33. **Khalid Eldwaib, Aleksandar Grbović, Gordana Kastratovic, Mustafa Aldarwish**, Design of wing spar cross section for optimum Fatigue life. Procedia structural integrity 13 (2018) 444-449.

Appendices

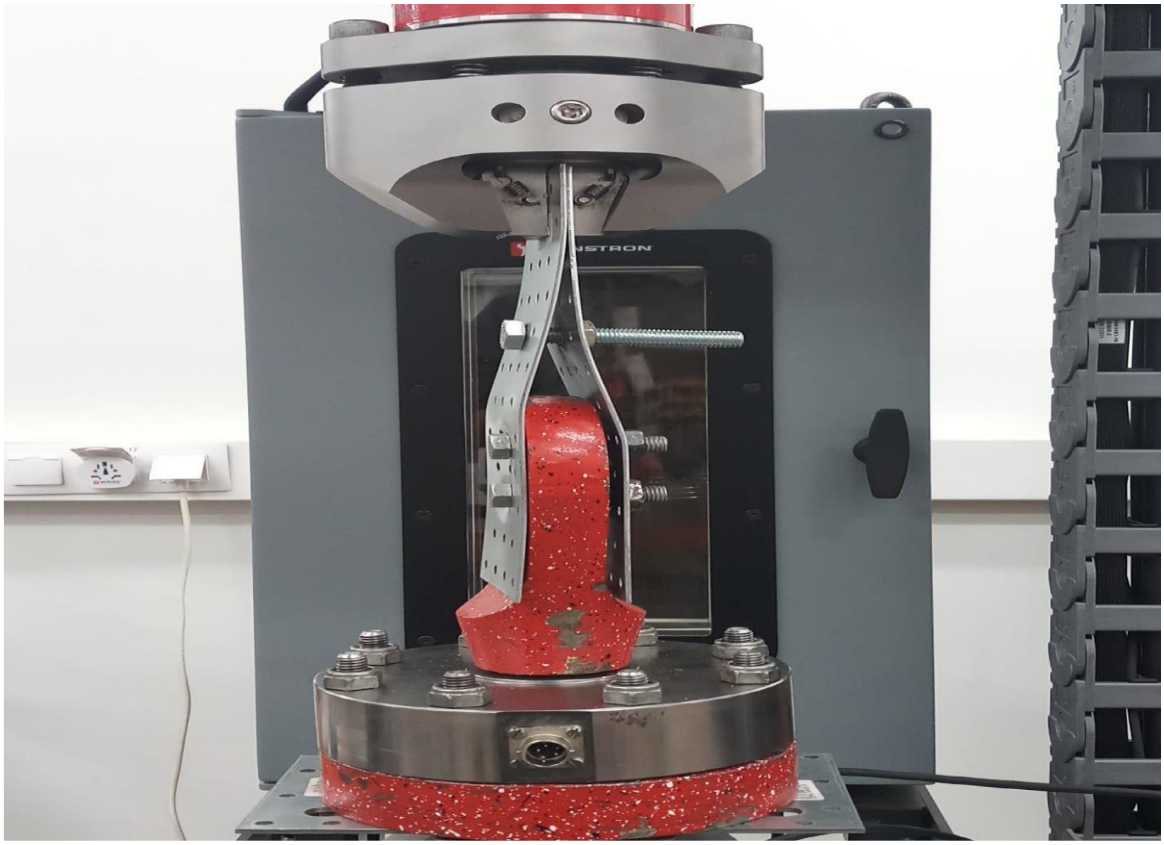

Figure. Calibration of the load cell (MK11-50KN)

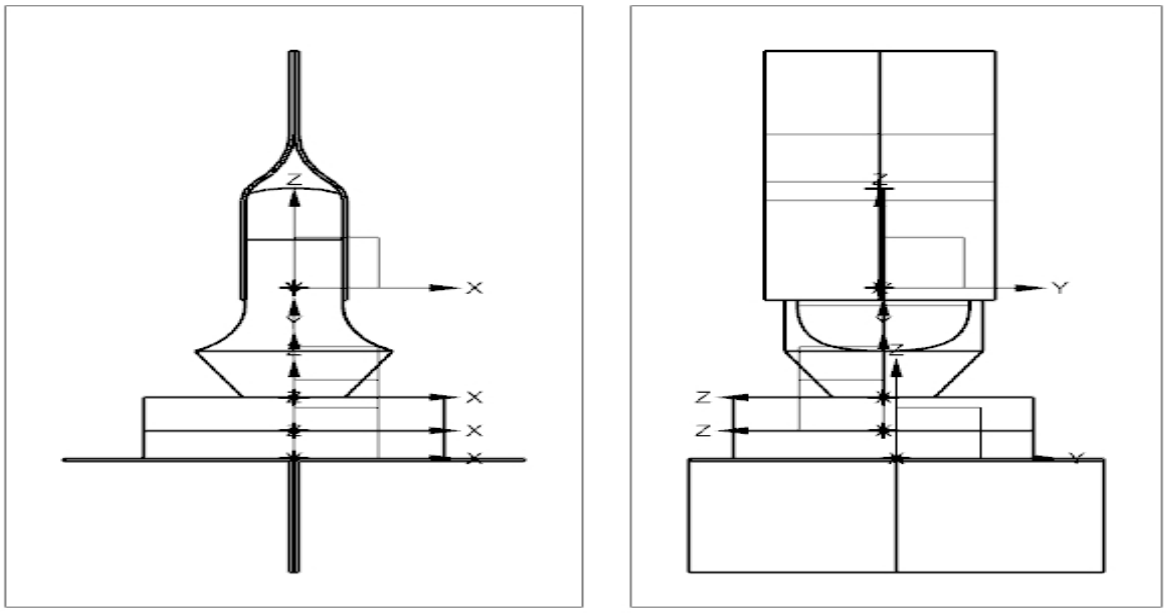

Figure. Drawing part of the load cell

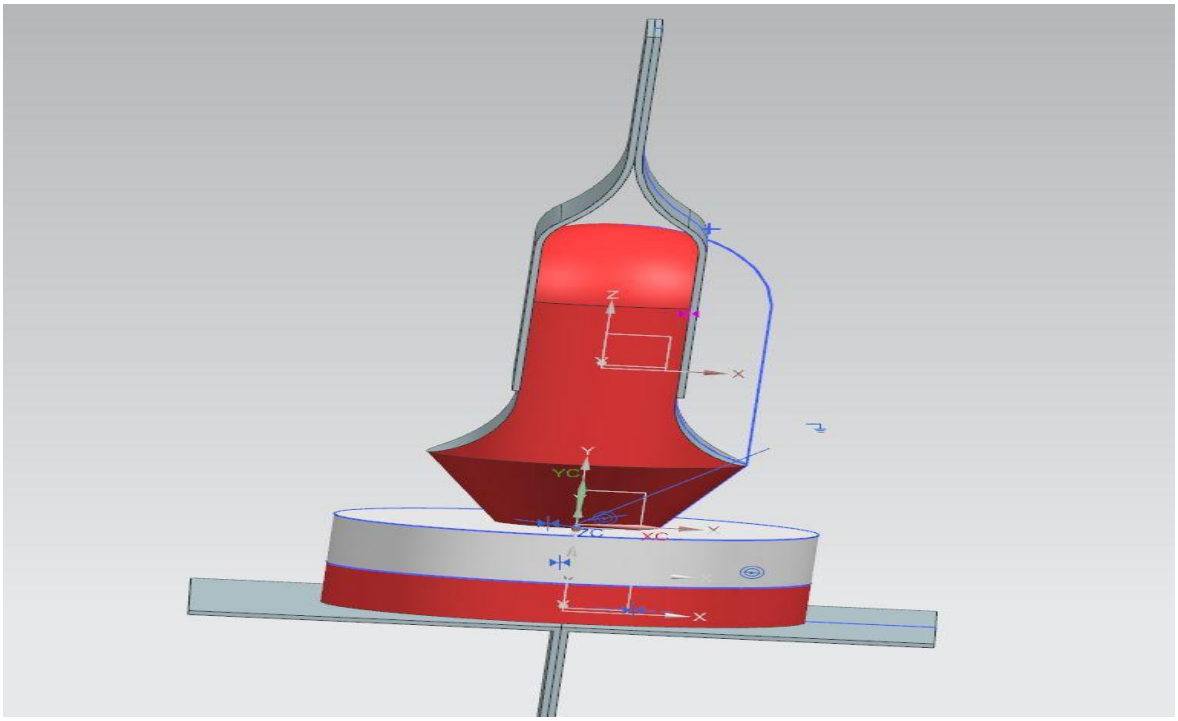

Figure. The design part of the load cell

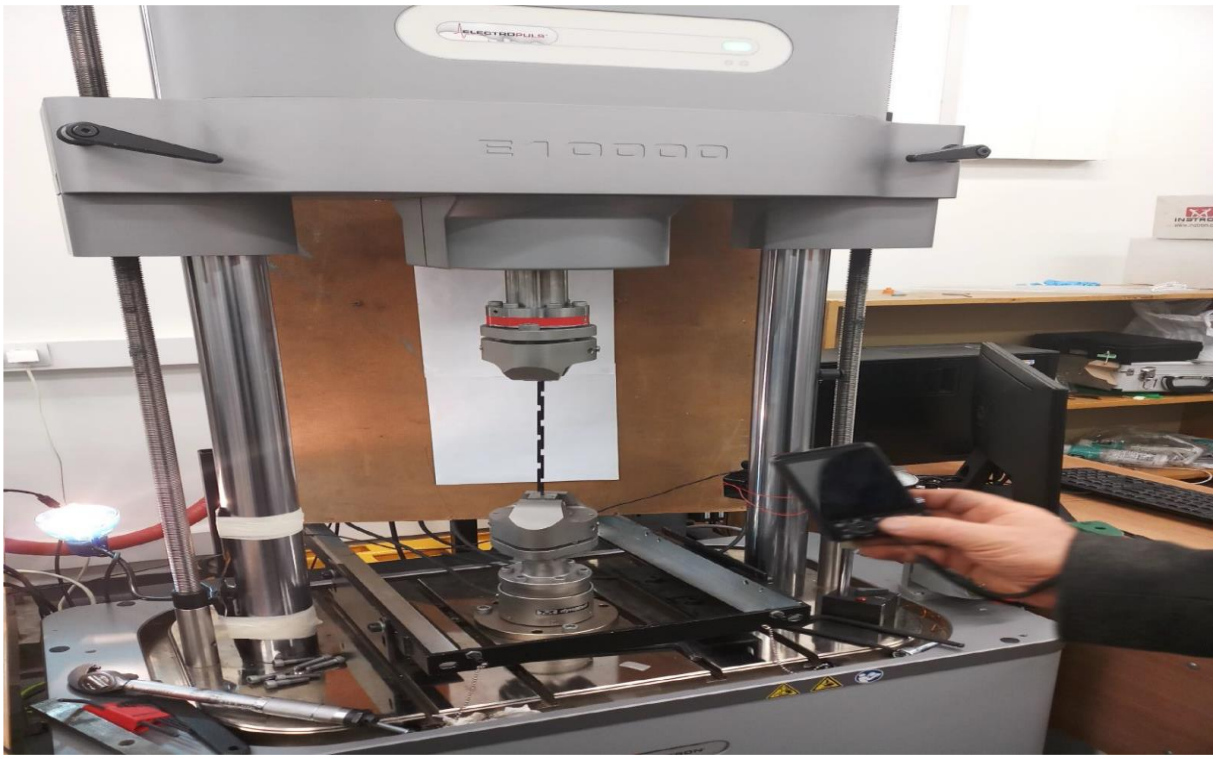

Figure. .Testing log chain specimen

Figure. Wing Locks

Figure. Experimental setup of a sailplane wing

Jaunųjų mokslininkų konferencija

pažymėjimas

PRA
MO inžinerija
NĖS
2018

Nr. V24-11-58

pažymime, kad 2018 m. gegužės 10 d.

Naga Manikanta Kommanaboina, Hari Prasanna Manimaran, Mastan Raja Papanaboina, Kazimieras Petkevičius

dalyvavo KTU Jaunųjų mokslininkų konferencijoje
„Pramonės inžinerija-2018" ir pristatė pranešimą

ANALYSIS OF ADHESIVE BONDING IN CARBON FIBER BAR SINGLE LAP JOINT

MIDF Dekanas dr. Andrius Vilkauskas

„Santakos" slėnis, Kaunas

organizatorius ktu mechanikos inžinerijos ir dizaino fakultetas 1922

partneris PTO PAKUOČIŲ TVARKYMO ORGANIZACIJA

23rd International Scientific Conference "MECHANIKA-2018"

18 MAY 2018, DRUSKININKAI, LITHUANIA

CERTIFICATE of Attendance

This Certificate of Attendance is given to

Naga MANIKANTA KOMMANABOINA

Kaunas University of Technology

for participating in the International Conference „Mechanika 2018".

Kaunas University of Technology
Lithuanian Academy of Science
IFToMM National Committee of Lithuania
Baltic Association of Mechanical Engineering

Scientific Secretary of the Conference
Saulius Diliūnas

International Young Scientists Conference

certificate

IND UST engineering RIAL 2019

Nr. V24-11-27

Atendence confirmation for

Naga Manikanta Kommanaboina

to certificy the presented theme

FINITE ELEMENT APPROACHES TO SIMULATE THE DIFFERENT TYPES OF SAILPLANE SPAR CONNECTION

at the International conference of Industrial Enginering,
17 May 2019, Kaunas, Lithuania

Dean of the Faculty of Mechanical
Engineering and Design
dr. Andrius Vilkauskas

Kaunas "Santaka" Valley
Kaunas University of Technology

organiser

ktu 1922 faculty of mechanical engineering and design

24th International Conference MECHANIKA '2019